LA-UR-80-2891

Conf-801011--54

TITLE: A MODIFIED WETTED-WALL INERTIAL FUSION REACTOR CONCEPT

AUTHOR(S): John H. Pendergrass
Thurman G. Frank
Ihor O. Bohachevsky

SUBMITTED TO: Fourth ANS Topical Meeting on
The Technology of Controlled Nuclear Fusion
King of Prussia, PA
October 14-17, 1980

MASTER

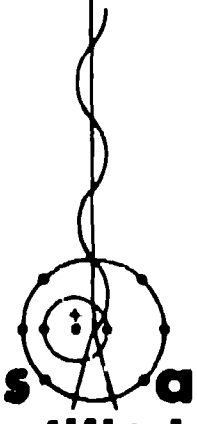

los alamos
scientific laboratory
of the University of California
LOS ALAMOS, NEW MEXICO 87545

Form No. 836
St. No. 2629
1/75

UNITED STATES
ENERGY RESEARCH AND
DEVELOPMENT ADMINISTRATION
CONTRACT W-7405-ENG. 36

Summary

Limitations on reactor pulse repetition rate and uncertainties with respect to assurance of first wall protection in LASL wetted-wall inertial fusion reactor concepts, in which restoration of cavity conditions to those required for acceptable driver energy pulse transmision following pellet microexplosion is accomplished by exhaust of ablated liquid metal through nozzles and protective films are formed by forcing liquid metals through porous first walls, can be circumvented through alternative methods of cavity clearing and protective film formation. Simple, exploratory analyses indicate that our modified wetted-wall concept, in which protective liquid metal films are injected directly onto cavity walls through slit nozzles to ensure first wall protection and are held there by centrifugal forces and cavity clearing occurs by condensation of vapor on film liquid not ablated as a result of pellet x ray and debris ion energy deposition, can be operated at substantially higher repetition rates. The new mode of operation appears to be attractive for heavy ion fusion, for which constraints on cavity design options may be more severe, as well as laser fusion. Numerical results of the exploratory analyses, plus discussion of aspects of the new concept requiring further work, are presented.

Introduction

The original Los Alamos Scientific Laboratory wetted-wall inertial fusion reactor concept for commercial applications[1,2] includes:

* protection of reactor cavity first walls from damage by soft x rays and pellet debris ions released by pellet microexplosions by thin liquid metal (lithium) films formed by forcing the liquid metal through porous metal liners and

* restoration of conditions (reduction in cavity atmosphere atom number density to an ill-defined critical value) necessary for transmission of driver (lasers or heavy-ion accelerators) energy pulses through the cavity from beam ports to pellets without unacceptable loss in quality (energy and focusability) by exhaust of vapor generated by ablation of the liquid metal protective films through a nozzle, ~~with a liquid metal spray condenser used to maintain a low pressure downstream of the nozzle~~.

Two primary potential shortcomings of this concept have induced us to examine a modification of the original wetted-wall concept: (1) limitations on reactor pulse repetition rates and (2) barriers to adaptation of wetted-wall reactors for use with heavy-ion drivers. There is also some concern about satisfactory long-term protection of first walls (integrity of the porous liner over extended periods of operation).

Therefore, we have performed an exploratory analysis of a modification of the original wetted-wall concept, illustrated schematically in Fig. 1, that involves:

* direct injection of protective liquid metal films through slit nozzles onto cavity first walls to provide positive coverage at a throughput sufficiently great that all fusion energy trapped in th cavity can be removed as sensible heat of the liquid ~~(supplemented by transfer through the first walls if desired)~~ with a modest temperature rise and

* clearing of vapor from cavities between pellet microexplosions by condensation onto liquid metal not evaporated as a result of x ray and pellet debris heating and removal through simple drains in the bottoms of the cavities.

Wetted-Wall Reactor Cavity Phenomenology

The sequence of events in a wetted-wall reactor cavity following a pellet microexplosion can be summarized as follows. Soft x-ray photons emitted by the expanding pellet debris plasma and the debris ions themselves, both of low penetrating power, deposit their energy in thin surface layers of the liquid metal films protecting cavity first walls over a very short time interval. If the films are thin, very little ~~fusion~~ neutron energy is deposited in them. Part ~~or all~~ of the liquid metal in the films is vaporized, heated to high temperature, and expands to fill the cavity. If the reactor has been supplied with an exhaust nozzle, ~~vapor is condensed downstream of the nozzle to maintain the flow,~~ and the walls of the reactor cavity are sufficiently hot, then vapor will leave the cavity through the nozzle without condensing. This means of restoration of original cavity conditions corresponds to the postulated mode of operation of the reference wetted-wall concept and involves extraction of fusion energy trapped in the cavity from the cavity as latent and sensible heat of the vapor.

If, on the other hand, there is no nozzle, but the cavity walls are cooled or cool liquid metal is pumped through the cavity at a sufficiently high rate, then the vapor will condense onto the cavity walls or liquid metal in the protective films that was not vaporized by the pellet microexplosion. Fusion energy trapped in the cavity is thus removed by conduction through the cavity walls or as sensible heat of the liquid. The latter of these two design options corresponds to the modified wetted-wall reactor concept to which we will devote most of our attention. ~~However, a combination of conduction through the wall and removal as liquid sensible heat could also be used to extract trapped fusion energy from the cavity.~~

The temperatures required to prevent all condensation of evaporated liquid metals seriously considered for fluid wall reactor applications are relatively high (too high, e.g., for steels) and the flow of new, cool liquid metal through porous first walls to form protective films is continuous. Therefore, the original wetted-wall concept must involve some condensation, as well as exhaust through a nozzle, ~~and must display some of the characteristics of the modified wetted-wall concept. In fact, as we shall demonstrate, condensation on liquid metal films on the cavity walls would probably be the dominant mechanism for vapor removal from reference wetted-wall cavities.~~

Wetted-Wall Reactor Cavity Phenomenology

The sequence of events in a wetted-wall reactor cavity following a pellet microexplosion can be summarized as follows. Soft x-ray photons emitted by the expanding pellet debris plasma and the debris ions themselves, both of low penetrating power, deposit their energy in thin surface layers of the liquid metal films protecting cavity first walls over a very short time interval. If the films are thin, very little ~~fusion~~ neutron energy is deposited in them. Part ~~or all~~ of the liquid metal in the films is vaporized, heated to high temperature, and expands to fill the cavity. If the reactor has been supplied with an exhaust nozzle, ~~vapor is condensed downstream of the nozzle to maintain the flow,~~ and the walls of the reactor cavity are sufficiently hot, then vapor will leave the cavity through the nozzle without condensing. This means of restoration of original cavity conditions corresponds to the postulated mode of operation of the reference wetted-wall concept and involves extraction of fusion energy trapped in the cavity from the cavity as latent and sensible heat of the vapor.

If, on the other hand, there is no nozzle, but the cavity walls are cooled or cool liquid metal is pumped through the cavity at a sufficiently high rate, then the vapor will condense onto the cavity walls or liquid metal in the protective films that was not vaporized by the pellet microexplosion. Fusion energy trapped in the cavity is thus removed by conduction through the cavity walls or as sensible heat of the liquid. The latter of these two design options corresponds to the modified wetted-wall reactor concept to which we will devote most of our attention. ~~However, a combination of conduction through the wall and removal as liquid sensible heat could also be used to extract trapped fusion energy from the cavity.~~

The temperatures required to prevent all condensation of evaporated liquid metals seriously considered for fluid wall reactor applications are relatively high (too high, e.g., for steels) and the flow of new, cool liquid metal through porous first walls to form protective films is continuous. Therefore, the original wetted-wall concept must involve some condensation, as well as exhaust through a nozzle, ~~and must display some of the characteristics of the modified wetted-wall concept. In fact, as we shall demonstrate, condensation on liquid metal films on the cavity walls would probably be the dominant mechanism for vapor removal from reference wetted-wall cavities~~.

flow of liquid metal through the cavities is great enough that the free surface temperature of the liquid metal remaining on cavity walls following pellet microexplosions rapidly relaxes to and remains at values low enough that driving forces for evaporation become negligible in comparison to driving forces for condensation.

* For conventional wetted-wall reactor cavities, a convergent-divergent nozzle with downstream pressure sufficiently low that flow through the throat is sonic at all times is used.

* For conventional wetted-wall reactors, condensation does not occur.

* Condensation and exhaust through nozzles can be approximated as quasi-static processes with acceptable accuracy.

* The liquid metal protective film surface area available for condensation in modified wetted-wall reactor cavities equals the first wall surface area (the effects of condensation to form drops, film fragmentation, surface waves, thick films, etc., that tend to alter surface area are negligible and beam ports, whose cumulative cross sectional area is only a few percent of the total first wall area, act as vapor sinks of capacity equivalent to liquid metal films of areas equal to their cross-sectional areas).

* Following cavity blowdown, the mass of vapor remaining in the cavity is negligibly small (low pressures).

* The criterion for acceptable driver energy pulse transmission through cavity atmospheres is reduction in vapor atom density to or below a critical value.

A mass balance for the vapor phase in the reactor cavities that encompasses both conventional and modified wetted-wall concepts can be expressed as:

(net rate of accumulation of mass in the vapor phase in the cavity) +
(net rate of removal of mass from the vapor phase in the cavity
through condensation on remaining liquid metal in protective films) +
(net rate of removal of mass from the vapor phase in the cavity by
flow through nozzles) = 0 (11)

The second term is zero for the conventional wetted-wall reactor cavity model defined above and the third term is zero for the modified wetted-wall model. The first term can be written as:

$$V_C \frac{d\rho}{dt} \quad (12)$$

where V_C, ρ, and t are respectively the reactor cavity volume, the uniform, quasi-steady density of vapor in the cavity, and time.

From simple ideal gas kinetic theory, the flux $\phi^{\pm}$ of molecules through a reference plane in either direction in a pure, uniform, quiescent gas is given by:

$$\phi^{\pm} = \rho \sqrt{\frac{RT}{2\pi M}} \quad (13)$$

where R, P, M, and T are respectively the ideal gas constant and the pressure, molecular weight, and absolute temperature of the gas. If there is a net current ϕ through the reference plane, then the flux $\phi^{\pm}$ through the plane in the direction of the current is given by:

$$\phi^{+} = \rho \sqrt{\frac{RT}{2\pi m}} f(\lambda) \quad (14)$$

where:

$$f(\lambda) = e^{-\lambda^2} + \pi^{1/2} \lambda [1 + \mathrm{erf}(\lambda)] \quad (5)$$

$$\lambda = \phi^+ / \rho \sqrt{\frac{2RT}{m}} \quad (6)$$

and $f(\lambda)$ is greater than one for ϕ^+ greater than zero.[3] Now

$$\phi = \phi^+ - \phi^- \quad (7)$$

Our model for cavity blowdown includes uniformity of the vapor phase remaining in the cavity at all times and negligibility of ϕ^- at liquid metal film surfaces at which condensation is occurring. Therefore, for our model the flux of molecules striking liquid metal film surfaces is given by:

$$\phi = \phi^+ = \rho \sqrt{\frac{RT}{2\pi m}} \quad (8)$$

If we denote the fraction of molecules striking the surface that actually condense, the so-called condensation or accomodation or sticking coefficient, by σ, then the rate of condensation in a modified wetted wall reactor cavity can be expressed as:

$$\sigma\phi = \sigma\rho \sqrt{\frac{RT}{2\pi m}} f(\lambda) \quad (9)$$

Existing theory for estimating σ is not considered reliable and experimental values for σ are scarce, with unambiguous measurements apparently performed only very recently. Because we have no experimental data for systems of potential interest for modified wetted-wall applications, we have used a value of one for σ, while being aware that reported values for some liquid metal systems are somewhat lower and apparently tend to decrease approximately linearly with decrease in temperature. For very rapid condensation, other effects will act to reduce condensation rates, but by taking $f(\lambda)$ σ as unity we believe that the above simple expression for the condensation rate in modified

wetted-wall reactors will be conservative or at worst will not seriously overestimate condensation rates.

The mass flow rate of vapor from a cavity through a nozzle at sonic velocity is given by the produce of vapor density ρ_T and vapor sonic velocity a_T in the nozzle throat and the cross-sectional area A_T of the throat. Vapor conditions in the nozzle throat can be related to quasi-equilibrium reservoir conditions for an ideal gas according to:

$$\rho_T = \left(\frac{2}{\gamma+1}\right)^{\frac{1}{\gamma-1}} \rho \qquad (10)$$

and:

$$a_T = \sqrt{\frac{2}{\gamma+1}}\, a \qquad (11)$$

where the sound speed in the vapor in the cavity a is given by

$$a = \sqrt{\frac{\gamma RT}{M}} = \sqrt{\frac{\gamma P}{\rho}} \qquad (12)$$

and γ is the ratio of specific heat at constant pressure c_p to the specific heat at constant volume c_v for the vapor.

The expressions for the three terms in the cavity vapor mass balance can be assembled to give:

$$V_C \frac{d\rho}{dt} + \alpha\rho \sqrt{\frac{RT}{2\pi m}} A_C \qquad (13)$$

$$+ \left(\frac{2}{\gamma+1}\right)^{\frac{1}{\gamma-1}} \sqrt{\frac{2\gamma}{\gamma+1}} \sqrt{P_v} = 0 \qquad (14)$$

For an ideal gas undergoing adiabatic, reversible expansion:

$$T = T_0 \left(\frac{\rho}{\rho_0}\right)^{\gamma-1} \qquad (15)$$

where the subscript o denotes initial values. Also, for an ideal gas:

$$\rho = \frac{MP}{RT} \qquad (16)$$

The cavity vapor mass balance can therefore be transformed nto a differential equation relating a single independent ariable and single dependent variable:

$$\frac{d\rho}{dt} + C\rho^{\frac{\gamma+1}{2}} / \rho_0^{\frac{\gamma+1}{2}} = 0 \qquad (17)$$

ere:

$$C = \sqrt{\frac{RT_0}{M}} \frac{A_C}{V_C} \left[\frac{1}{2\pi} + \frac{A_T}{A_C} \left(\frac{2}{\gamma+1} \right)^{\frac{1}{\gamma-1}} \sqrt{\frac{2\gamma}{\gamma+1}} \right] \qquad (18)$$

e solution to this equation that satisfies the initial ndition:

$$\rho = \rho_0, \quad t = 0 \qquad (19)$$

:

$$\rho = \rho_0 / (1 + \frac{\gamma-1}{2} Ct)^{\frac{2}{\gamma-1}} \qquad (20)$$

s result can be transformed into equations giving cavity osphere pressure and temperature as functions of time:

$$T = T_0 / (1 + \frac{\gamma-1}{2} Ct)^2 \qquad (21)$$

$$P = \frac{\rho_0 RT_0}{M} \Big/ \left[1 + \frac{\gamma-1}{2} C \right]^{\frac{2\gamma}{\gamma-1}} \qquad (22)$$

number of moles m and number density N of vapor in the ty as a function of time can be computed using the ective relations:

$$m = \frac{\rho V_C}{M} \qquad (23)$$

and:

$$N = \frac{N_{Av}\rho}{M} \qquad (24)$$

where N_{AV} is Avogadro's number.

The time t* required for the cavity vapor number density to fall to the critical value N* required for acceptable transmission of driver energy pulses following pellet microexplosions is obtained by inverting Equation 20 and combining with Equation 24 to arrive at:

$$t^* = \left[\left(\frac{N_{Av}\rho_0}{MN^*}\right)^{\frac{\gamma-1}{2}} - 1\right] \Big/ \left(\frac{\gamma-1}{2}\right), C \qquad (25)$$

For cavity clearing by exhaust through a nozzle C reduces to:

$$C_N = \left(\frac{2}{\gamma+1}\right)^{\frac{1}{\gamma-1}} \sqrt{\frac{2\gamma}{\gamma+1}} \sqrt{\frac{RT_0}{M}} \frac{A_T}{\sqrt{V_C}} \qquad (26)$$

and for clearing by condensation C becomes:

$$C_C = \sqrt{\frac{RT_0}{M}} \frac{A_C}{V_C} \qquad (27)$$

The ratio of cavity blowdown time for the modified wetted-wall concept to that for the conventional wetted-wall concept is simply:

$$1/C_C \Big/ 1/C_N = \left(\frac{2}{\gamma+1}\right)^{\frac{1}{\gamma-1}} \sqrt{\frac{2\gamma}{\gamma+1}} \frac{A_T}{A_C} \qquad (28)$$

We see that, except for the factor:

$$\left(\frac{2}{\gamma+1}\right)^{\frac{1}{\gamma-1}} \sqrt{\frac{2}{\gamma+1}} \qquad (29)$$

which has the respective values 0.726 and 0.685 for monoatomic ($\gamma = 5/3$) and diatomic ($\gamma = 7/5$) ideal gases, the ratio of blowdown times is given by the ratio of nozzle throat area to cavity first wall area. Because:

$$A_T/A_C << 1 \qquad (30)$$

i.e., typically less than 0.1, cavity clearing times when condensation is the mechanism by which vapor is removed are much less than when exhaust through supersonic nozzles is the mode of cavity clearing, everything else being equal. It is also interesting to note that according to Eq. (25), t^* decreases with increase in T_o, P_o, r_o, γ, V_c, N^*, and A_T/A_C respectively when all other parameter values are held constant.

Prediction of the exact amount of vapor generated by a pellet microexplosion is still problematical and the application of our best available tools to this problem requires considerable resources. Therefore for the present we have parameterized the problem. The slower-moving pellet debris ions are expected to encounter liquid metal ablated by the faster-moving x-ray photons and deposit at least a substantial fraction of tneir kinetic and excitation energy in vapor. X-ray energy may similarly be partitioned between vapor sensible heat and latent heat of vaporization. We project that liquid sensible heat effects due to pellet soft x-rays and debris ions prior to condensation of evaporated material will be small and therefore we neglect pellet x-ray and debris ion energy that does not initially go into evaporation of liquid and heating of the vapor. The modest amount of volumetrically deposited ~~fusion~~ neutron and hard x-ray energy will play a negligible role in forming and heating vapor. If the partition between heat of vaporization and vapor sensible heat is expressed in terms of the fraction f_V that goes into vaporization and Y_{XD} represents the fusion energy release per microexplosion that appears as soft x-ray and ion energy emissions, ~~by the expanding plasma resulting from pellet burn~~,

then the moles n_o of protective film liquid metal evaporated per microexplosion and the temperature T_o to which the vapor is heated are given by:

$$n_o = \frac{f_V Y_{XD}}{\Delta H_V} \qquad (31)$$

and:

$$T_o = T_V + \frac{\Delta H_V}{c_v} \frac{1-f_V}{f_V}$$

$$- \frac{\Delta H_V}{c_v} \frac{1-f_v}{f_V} \text{ for } T_o >> T_V \qquad (32)$$

where ΔH_V, c_v, and T_V are respectively the heat of vaporization, the molar specific heat of the vapor, and the temperature at which the vapor is generated. We use representative average values for these properties. The amount of vapor formed per pellet microexplosion can also be expressed in terms of a vapor density:

$$\rho_o = \frac{f_V Y_{XD} M}{\Delta H_V V_c} \qquad (33)$$

and the corresponding pressure is given by:

$$P_o = \frac{RT_o}{M} \rho_o \qquad (34)$$

For a particular commercial applications pellet design inertial fusion reactor cavity first wall area is often scaled with pellet yield. We have adopted this convention and therefore we have:

$$A_C = k Y_{XD} \qquad (35)$$

where k is a constant of proportionality,

and, if geometric similitude is maintained when scaling, then:

$$V_C = G\,(k\,Y_{XD})^{3/2} \qquad (\cdot\cdot)$$

where G is a geometry factor. G has the form:

$$G = (3\sqrt{4\pi})^{-1} \qquad (3\cdot)$$

for spherical reactor cavities and:

$$G = \left(2^{3/2}\sqrt{\pi\zeta}\right)^{-1} \qquad (\cdot\cdot)$$

for cylindrical cavities, where ζ is the ratio of cavity length to cavity diameter.

Substitution of these results into our expression for the clearing time gives us:

$$t^* = \left[\left(\frac{N_{Av} f_V Y_{XD}}{N^* \Delta H_V \frac{V}{C}}\right)^{\frac{\gamma-1}{2}} - 1\right] \Big/ \left(\frac{\gamma-1}{2}\right) C \qquad (34)$$

where for the case of exhaust through a nozzle:

$$C_N = \frac{\left(\frac{2}{\gamma+1}\right)^{\frac{1}{\gamma-1}} \sqrt{\frac{2\gamma}{\gamma+1}}}{\sqrt{\frac{R}{M}\left(T_V + \frac{\Delta H_V}{C_V}\frac{1-f_V}{f_V}\right)}\, G\,(kY_{XD})^{3/2}} \qquad (40)$$

and for cavity clearing by condensation:

$$C_C = \sqrt{\frac{R}{M}\left(T_V + \frac{\Delta H_V}{C_V}\frac{1-f_V}{f_V}\right)} \Big/ G\sqrt{kY_{XD}} \qquad (41)$$

transmissivity

Analysis of wetted-wall reactor cavity blowdown

Exact analysis of the complex phenomena in wetted-wall reactor following pellet microexplosions is not presently possible. Present limitations have prevented thorough analysis within present capabilities. Therefore, we have contented ourselves for the present with the following approximate, suggestive analysis for the time required for restoration of reactor cavity atmosphere conditions (pressure following pellet burn) to those necessary for transmission of the next driver energy pulse through the cavity to the next injected pellet with an acceptable amount of degradation in beam quality. This time is expected to largely determine maximum reactor pulse repetition rate.

Our analysis was conducted using a rigid, simplified model defined by the following assumptions and approximations:

* After a time interval following pellet microexplosions that is short in comparison to the time interval between microexplosions, liquid metal evaporated from protective films on cavity walls relaxes into a uniform, quasi-equilibrium state.

* The vapor phase obeys the ideal gas law at all times.

* Vapor remaining in the cavity expands adiabatically and reversibly.

* The use of constant, representative mean values of thermophysical properties will result in acceptable accuracy.

* The effects of substances other than evaporated liquid metal, e.g., pellet debris, on blowdown phenomena are negligible and the vapor composition is the same as that of the liquid.

* For modified wetted-wall reactor cavities, thermal transport through protective liquid metal films is sufficiently rapid and the rate of

ie can now deduce that t^* decreases with increase in T_v although the effect is minor because typically $T_o >> T_v$), nd ΔH_v, and increases with increase in c_v, ρ_v, and $(\gamma - 1)$ XD'

In order to generate specific results using the preceding heory, we have investigated the use of lithium as the rotective liquid metal in spherical reactor cavities. We have lso introduced an additional simplifying approximation: ithium vapor is taken to be entirely monoatomic, rather than ily mostly monoatomic. The values that we have used for T_v, c_v, ΔH_v, and γ are respectively 1000 K, 25.0 J/mol K, .58 x 10^5 J/mol, and 1.67. Some results of our parameter udies are summarized in Figs. 2 and 3. The most important plication of these numerical results is a reinforcement of ir earlier claim that removal of evaporated protective liquid tal from wetted-wall reactor cavities can be accomplished ch more rapidly by condensation than by exhaust through a zzle.

Liquid Metal Allowable Temperature Rise and Required Throughput and Alternatives to Lithium

In general, there are upper and lower operating temperature limits for wetted-wall inertial fusion reactor cavities. The melting point (e.g., 459 K for lithium) of the liquid metal used for first wall protection, plus a reasonable safety margin, determines the lower limit.

The upper limit is determined by cavity conditions required for transmission of driver energy pulses through cavity atmospheres ~~to pellet~~ with acceptable degradation. In general, these conditions are not well established, but are typically characterized simply in terms of estimated upper limits on species-dependent cavity atmosphere atomic number densities. For, e.g., lithium cavity atmospheres, the estimated critical atom number density for acceptable transmission of CO_2 laser light pulses of the pulse durations (~ 1 ns) and total energies (~ 1 to 10 MJ) required for commercial applications is estimated at 10^{15}/cm. Acceptable focusing and propagation of heavy ion pulses through cavity atmospheres may be possible only for number densities as low as 10^{12}/cm , which corresponds to ~ 10^{-4} torr cavity atmosphere pressures. Thus, an upper limit on cavity operating temperature is determined by the vapor number density in thermal equilibrium with liquid metal leaving reactor cavities. In practice, the protective film liquid must exit cavities at somewhat lower temperatures.

Experimental values for Li and Li_2 partial pressures and derived total lithium atom number densities in equilibrium with the liquid are displayed in Fig. 4. Thus, the inlet temperature of lithium used for first wall protection in wetted-wall inertial fusion reactor cavities must be greater than ~ 510 K (the melting temperature plus ~ 100 K). Its outlet temperature cannot exceed ~ 810 K (the temperature corresponding to an equilibrium lithium atom vapor number density of $10^{15}/cm^3$ minus ~ 100K) if a CO_2 laser driver is to be employed. If a heavy ion driver is to be accomodated and the critical number density is $10^{12}/cm^3$, then with a 100 K safety margin, the lithium outlet temperature

would be ~ 525K. In the CO_2 laser case, the permissible temperature rise of the lithium is thus ~ 300 K, whereas, unless one or both of the safety margins are reduced, the allowable temperature rise with heavy ion drivers is discouragingly small, i.e., only ~ 15 K. The large liquid metal circulation rates implied by such small temperature rises mean large pumping power requirements

The above result for heavy ion drivers is one reason why the use of alternative liquid metals with lower vapor pressures than lithium in the temperature range up to ~ 1000 K are being considered for first wall protection in wetted-wall reactors adapted for use with this class of drivers. The liquid metal in fluid-wall reactors that employ thick layers to reduce neutron, as well as x ray and ion, damage to first walls must still contain lithium for tritium breeding purposes. Thus, severely restrictions on the choice of protective liquid-metal systems in ssuch reactors. The thin protective liquid-metal films in wetted-wall reactors need not breed tritium and therefore any liquid metal suitable on other grounds can be used for first wall protection in this class of reactors. Furthermore, while the blanket must breed tritium to close the tritium fuel cycle, the blanket need not contain a liquid metal and can operate at substantially different temperature and pressure levels. Even if the low cavity vapor density requirements currently projected for heavy ion drivers prove to be unnecessary, the separation of first wall protection and tritium breeding functions could turn out to be important for successful commercialization of inertial fusion with laser, as well as heavy ion, drivers.

Even if allowable temperature rise considerations are not significant for a particular liquid metal, higher operating temperature levels can result in more efficient utilization of fusion energy and, e.g., less expensive electric power, if the cost of materials required for alternative liquid metal containment and circulation at higher temperatures are not excessive compared to lower-temperature operation with lithium. Favorable characteristics of liquid metals for first wall protection in wetted-wall reactors, in addition to a large allowable temperature rise and a low melting point, include high liquid thermal conductivity and specific heat capacity, low liquid viscosity and density, low vapor specific heat and high ratio of vapor

specific heat capacity at constant pressure to specific heat capacity at constant volume (e.g., monoatomic rather than polyatomic vapors), and a high molar heat of vaporization. The liquid properties determine heat transfer and transport characteristics and pumping power requirements. The remainder affect cavity clearing times and hence reactor pulse repetition rate.

Alternatives to lithium that have been suggested for use in wetted-wall reactors include various lead/lithium mixtures (e.g., 83 at % lead, MP ~ 533 K, 10^{-4} torr vapor pressure ~ 930 K), the lead/bismuth eutectic (~ 44 at % Pb, ~ 398 K, ~ 860 K), and tin (~ 505 K, ~ 1090 K). In general, these alternatives exhibit physical property values that are less favorable than those of lithium, except for higher upper operating temperatures, resulting in higher pumping power requirements, less efficient heat transfer, and slower cavity clearing. In particular viscosities and densities of the liquid are greater, liquid specific heat capacities and thermal conductivities are lower, vapor specific heat capacities are higher and molar heats of vaporization are lower. Melting points for some of these alternatives are only moderately higher than for pure lithium, while for others, melting points are substantially lower. Thus, the lower operating temperature limits and allowable temperature rises for these liquid metals in wetted wall reactor cavities are acceptable.

The throughput of liquid metal required to remove all pellet energy release and neutron interaction energy trapped in reactor cavities can be expressed as:

$$\dot{m} = \dot{V}\rho_L = \frac{\nu Y_T}{c_L \Delta T_A} \qquad (42)$$

where $\dot{m}$, $\dot{V}$, Y_T, c_L, ρ_L and ΔT_A are respectively the mass and volume throughputs of liquid metal, trapped energy per pellet microexplosion, the specific heat capacity and density of the liquid, and the mean rise in temperature permitted the liquid in passing through the cavity. For example, for a 200-K temperature rise in a wetted-wall cavity operated at 10 hertz and trapping 50 MJ per pellet microexplosion in the cavity with lithium (with ρ_L = 0.494 g/cm^3 ~~at the temperature~~ and an average value for c_L of 4.18 J/gK) as the liquid metal, we have values of 399 kg/s and 0.81 m^3/s respectively for $\dot{m}$ and $\dot{V}$. Neither of these values is particularly large.

Hydrodynamics and Stability of Protective Liquid Metal Films

The hydrodynamics of protective liquid metal films that are bombarded with pulsed radiation of both limited (soft x rays and pellet debris ions) and substantial (neutrons and hard x rays) penetrating power will be complex. Pulsed near-surface soft x-ray and pellet debris energy deposition resulting in surface ablation, followed by subsequent condensation, pulsed nonuniform hard x-ray and neutron volumetric energy deposition that may generate significant shock waves, and possible vibration of cavity first walls will act to disrupt such films. Centrifugal forces (when first walls are curved in the direction of flow) and forces developed by ablation, condensation currents, and high gas pressures during part of cavity cycles may aid in preserving the films and forcing them to remain on cavity walls. Our present understanding of the complex phenomena involved and available resources do not permit accurate analysis of film flow under these conditions. Therefore, we have concentrated on analyses of what is required to completely restore the films, assuming complete disruption, between successive pellet microexplosions and to provide the thermal energy transport capacity required to remove pellet x ray, debris ion, and neutron energy trapped in reactor cavities. In the process, various details of steady film flow have been examined by analyzing a simple model of the flow. We have confined our attention for the present to spherical reactor cavities with tangential, downward injection of liquid metal through horizontal, circular-slit nozzles located at specified angular distances from the top (upper pole) of the cavities. The injected liquid metal exits through drains in the bottoms of the cavities.

As we discuss in a subsequent section of this report concerned with protection of injection nozzles and admission of laser beams and recoverage of cavity walls after each microexplosion, we consider it likely that injection nozzles at only a single location will not be satisfactory in all instances. In addition, other cavity geometries, especially cylindrical, may

also be of interest. If vertical cylindrical cavities are of interest, the only way to use centrifugal force to aid in holding protective films on first walls is to inject fluid in a tangential partially horizontal direction, whereas with horizontal cylindrical cavities, directly downward injection can be used. However, at present we do not have definitive results to establish the importance of the contributions of centrifugal forces to satisfactory operation of the concept and may be guilty of overemphasizing their importance. In any event, film flows in cavities with different geometries and with multiple injection nozzles involve the same basic principles and can presumably be attacked by the same methods.

Our analysis of the protective liquid-metal film flow in modified wetted-wall reactor cavities is based on a number of simplifying assumptions and approximations:

* The film flow is everywhere fully-developed, turbulent, steady, and one-dimensional. In particular, the distance in the direction of flow from the injection nozzle required for change from the turbulent velocity profile in the injection nozzle to that of the wall jet is small and/or the difference between the two is small. Also, second-order effects due to changes in flow path width, curvature of the reactor cavity first wall, and slowing down and thickening of the film along the flow path are neglected. Changes in flow path width, except where diversion around beam ports, which we will discuss later, is required, may not be a significant consideration for cylindrical cavities. Effects of curvature of reactor cavity first walls on film flow will not generally be of much concern for the thin films under consideration.

* Friction factors and velocity profiles derived from pipe flow experiments can be adapted to accurately predict wall jet friction factors and velocity profiles.

* Shear stress at the free surface of the film can be neglected, a very good approximation when vapor densities are low.

* Changes in important, physical property values along the film in the direction of flow can be neglected, e.g., because the film is very nearly isothermal during the portions of the reactor cycle for which the analysis is intended to be applicable, or, alternatively, the use of representative constant average values of the physical properties will not introduce unacceptable error into the analysis.

The geometry of the model is illustrated schematically in Fig. 5.

A simple, but accurate, fully-developed, turbulent, time-averaged velocity profile model based on the results of pipe flow experiments was adapted for the present wall-jet analysis by substitution of the film thickness for pipe radius:

$$v(x,\theta) = v_M(\theta) \left[\frac{x}{\delta(\theta)}\right]^{1/n\left[N_{Re}(\theta)\right]}$$

where $v(x,\theta)$, $v_M(\theta)$, $\delta(\theta)$, and $n(N_{Re}(\theta))$ are respectively the time-smoothed velocity parallel to the solid surface as a function of distance x from the solid surface and angular position θ from the upper pole of the spherical reactor cavity, the angular position-dependent (or local) maximum film velocity (at the free surface of the film), the local film thickness, and the so-called flow index, a function of the local film Reynolds number $N_{Re}(\theta)$, defined as:

$$N_{Re}(\theta) = \frac{\bar{v}(\theta)\,\delta(\theta)}{\nu_L} \qquad (44)$$

where ν_L is the kinematic viscosity of the liquid and $\bar{v}(\theta)$ is the angular position-dependent time-smoothed average (over the film thickness) velocity. Some values of the function $n(N_{Re}(\theta))$ are listed in Table I .

The correlation:

$$f^{-1/2}(\theta) = 0.8686 \ln [2\delta(\theta)/\epsilon] -$$

$$0.8686 \ln [1 + 4.64\, e\, N_{Re}(\theta)\, f^{1/2}(\theta)/\delta(\theta)] + 1.14$$

$$= 0.8686 \ln [\delta(\theta)/e] -$$

$$0.8686 \ln [1 + 9.28\, n_L/ev(\theta) f^{1/2}(\theta)] + 1.14 \qquad (45)$$

for [illegible]riction factor $f(\theta)$ as a function of Reynolds number, film th[illegible] and equivalent sand roughness e was adapted from a very accurate empi[illegible]al correlation for flow in artificially roughened pipes[6] by replacing pipe radius with film thickness. The equivalent sand roughness can be interpreted as a height characteristic of solid surface roughness elements and is obtained for pipes constructed of a specified material by

comparing experimental friction factor values for these pipes with those measured under identical conditions in pipes artificially roughened with sand particles of known, uniform size attached to the pipe walls by adhesives. Representative values of e for common pipe materials of construction are listed in Table II.

Mass conservation for the liquid metal protective film can be expressed in the form:

(local flow path width)(local film thickness)(local average velocity) = (constant)

or:

$$[2\pi R\sin(\theta)][\delta(\theta)][\rho_L \bar{v}(\theta)] = [2\pi R \sin(\theta_o)\delta(\theta_o)\rho_L \bar{v}(\theta_o)] \qquad (47)$$

where the subscript o denotes conditions at the point of injection of the film and ρ_L is liquid density. Conservation of momentum in the direction of flow for an element of film lying between the angular positions θ and $\theta + \Delta\theta$ can be formulated as:

(net rate of accumulation of momentum within element) + (net rate of convection of momentum from element) = (summation of forces acting on fluid within element) (48)

Because the flow, although a function of angular position, is steady, the first term in this momentum balance is zero. The second term on the right hand side is given by:

$$2\pi R \sin(\theta) \int_0^{\delta(\theta)} \rho_L v^2(\theta,x)\,dx\Big|_{\theta+\Delta\theta} - 2\pi R \sin(\theta) \int_0^{\delta(\theta)} \rho_L v^2(\theta,x)\,dx\Big|_{\theta} \qquad (49)$$

The forces acting on the fluid within the element are components of the body force gravity in the direction of flow that acts throughout the element to

drive the flow and the surface friction force which acts at the film/first wall boundary to oppose the flow. These two forces give rise to the respective terms:

$$[\rho g \sin(\theta)]\,[2\pi R \sin(\theta)\,\delta(\theta) R\Delta\theta]\,\Big|_{\theta + \Delta\theta/2} \tag{50}$$

and:

$$-[2\pi R \sin(\theta)\, R\Delta\theta]\,[\tau_W(\theta)]\,\Big|_{\theta + \Delta\theta/2} \tag{51}$$

on the right hand side of the momentum balance, where g is the acceleration of gravity and $\tau_W(\theta)$ is the local momentum flux or shear stress at the fluid/solid interface. Combination of the various terms, rearrangement, and the taking of limits as approaches zero results in.

$$\frac{d}{d\theta}\left[\sin(\theta)\int_0^{\delta(\theta)} v^2(\theta,x)\,dx\right] = g R \sin^2(\theta)\delta(\theta) - \frac{R}{\rho_L}\sin(\theta)\tau_W(\theta) \tag{52}$$

for the momentum balance.

The integral in the preceding equation can be evaluated as follows. First we note that:

$$\int_0^{\delta(\theta)} v^2(\theta,x)\,dx = \frac{n(N_{Re}(\theta))}{n(N_{Re}(\theta))+2}\, v_M^2(\theta)\,\delta(\theta) \tag{53}$$

and that:

$$\bar{v}(\theta) = \frac{1}{\delta(\theta)}\int_0^{\delta(\theta)} v(\theta,x)\,dx = \frac{n(N_{Re}(\theta))}{n(N_{Re}(\theta))+1}\, v_M(\theta) \tag{54}$$

so that:

$$\int_0^{\delta(\theta)} v^2(\theta,x)\,dx = \frac{[(N_{Re}(\theta))+1]^2}{n(N_{Re}(\theta))[n(N_{Re}(\theta))+2]}\,\delta(\theta)\bar{v}^2(\theta) \tag{55}$$

The variation of the function of $n(N_{Re}(\theta))$ on the right hand side of t is relation with variation in $N_{Re}(\theta)$ is also indicated in Table 1. We see that this factor is very nearly constant and that setting it equal to a representative constant value K represents a useful approximation, which we have adopted, that will not introduce significant inaccuracy into the analysis. Also, by definition:

$$\tau_w(\theta) = [1/2\ \rho_L\ \bar{v}^2(\theta)]\ [f(\theta)] \qquad (56)$$

Thus, we have approximately for the momentum balance:

$$\frac{d}{d\theta}\left[\sin(\theta)\ \delta(\theta)\ \bar{v}^2(\theta)\right] = \frac{gR}{K}\sin^2(\theta)\delta(\theta) - \frac{k}{2K}\sin(\theta)\ \bar{v}^2(\theta)f(\theta) \qquad (57)$$

where $f(\theta)$ is obtained by solving the friction factor correlation. The continuity equation can be used to eliminate $\delta(\theta)$ from the momentum balance and the friction factor correlation to give respectively:

$$2\bar{v}(\theta)\frac{d\bar{v}(\theta)}{d\theta} = \frac{2gR}{K}\sin(\theta) - \frac{R}{K\sin(\theta_0)\delta(\theta_0)\bar{v}(\theta_0)}\sin(\theta)\,\bar{v}^3(\theta)f(\theta) \qquad (58)$$

and:

$$f^{-1/2}(\theta) = 0.8686\ln\left[2\sin(\theta_0)\delta(\theta_0)\bar{v}(\theta_0)/e\sin(\theta)\bar{v}(\theta)\right] - 0.8686\ln\left[\frac{1}{D} + 9.28(N_L/e\,\bar{v}(\theta)\,f^{1/2}(\theta)\right] + 1.14 \qquad (59)$$

The substitution:

$$\phi(\theta) = \bar{v}^2(\theta) \qquad (60)$$

then leads to:

$$\frac{d\phi(\theta)}{d\theta} = c_1 \sin(\theta) - c_2 \sin(\theta)\, \phi^{3/2}\, f(\theta)$$

and:

$$f^{-1/2}(\theta) = 0.8686 \ln [2 \sin(\theta_0)\delta(\theta_0)\bar{v}(\theta_0)/e \sin(\theta)\phi^{1/2}(\theta)] -$$
$$= 0.8686 \ln [1 + 9.28\, N_L/e\phi^{1/2}(\theta)\, f^{1/2}(\theta)] + 1.14$$

A FORTRAN computer program called LMFILMS has been written to integrate this differential equation using the fourth-order Runge-Kutla method. Newton-Rapheson interation is used to solve the friction factor equation. The output of the program includes local film thickness, average velocity, Reynolds number, friction factor, and time for a fluid element travelling at the local average (across the film thickness) velocity to move from the location of the injection nozzle to any angular position as functions of angular position on the first wall. The sensitivities of protective film flow characteristics to variations in reactor cavity radius, injection velocity, initial film thickness, location of the injection nozzle, and the roughness of the first wall surface have been investigated for lithium at 600 K (n_L = 0.006895 cm^2/s). Some results of these parameter studies are presented in Figs. 6-9. It must be recognized that at some point near the bottom of the spherical cavity as the film becomes very thick and the liquid metal more properly viewed as constituting a shallow pool, the model used in the analysis is no longer valid. However, it should also be recognized that at this point film stability, first wall coverage, etc., probably are no longer in doubt.

The injection velocity required for complete reformation of a protective film over the upper portion of a spherical reactor cavity between the angular position of injection θ_0 and another angular position θ following each pellet microexplosion can be estimated as follows. We approximate the film flow during the reestablishment period by the fully-developed, steady flow described above. The angular distance travelled by a fluid element moving everywhere at the local average film velocity in a time equal to the fraction f_ν of the intermicroexplosion time $1/\nu$ available for film reestablishment is given by:

$$R \int_{\theta_0}^{\theta} \frac{d\theta}{\bar{v}(\theta)} = \tau_{vv} = \tau_R(\theta)$$

The function $\tau_R(\theta)$ is plotted in Fig. 6. An upper bound on the angular distance over which the film is reestablished during the specified fraction of the period between pellet microexplosions can be estimated according to:

$$R \int_{\theta_0}^{\theta_0} \frac{d\theta}{v_M(\theta)} = f_{vv}$$

However, as noted previously:

$$v_M(\theta) = \frac{n(N_{Re}(\theta))+1}{n(N_{Re}(\theta))} \bar{v}(\theta)$$

and the value of the factor containing $n(N_{Re}(\theta))$ varies by only a few percent from 0.9 in the Reynolds number range of interest. Thus, the upper bound differs from the more conservative estimate by only about 10%.

The question of stability of protective liquid metal films perturbed by pellet emissions in modified wetted-wall reactor cavities will be extremely difficult to answer using present theory and computational tools. Resort to experiment will probably be necessary. We are not concerned here with more familiar instabilities such as transition from laminar to turbulent flow, free surface waviness, et ., and have no doubt that first wall coverage can be maintained with films of the type under consideration provided they are not perturbed. Instead, we are interested in whether or not the films will separate from cavity walls and fragment as a result of the impulses generated by x-ray, pellet debris ion, and neutron energy deposition, ablation from film free surfaces, and wall vibration. We have already listed the forces that may aid in preserving film integrity. Undisturbed films become very thick at the bottom of spherical cavities and we do not expect complete disruption of the films over the bottom portions of spherical cavity first walls. If any portion of the first wall is uncovered by pellet microexplosions, then the protective film in this region must be

reconstituted before the next pellet burn if excessive rates of damage to the first wall is to be avoided. If recoverage of the entire first wall is required after each pellet microexplosion, then the results in Fig. 5-6 indicate that undesirble limitations may be imposed on reactor pulse repetition rates unless multiple injection nozzle locations are used. In addition, severe fragmentation of protective film liquid or condensation to form droplets could result in formation of an aerosol that is difficult to clear rapidly from reactor cavities. This latter possibility, which has as yet not been investigated in a definitive way, is common to all fluid-wall inertial fusion reactor concepts.

However, we are optimistic that the fast-moving, relatively thick films under consideration will be relatively stable, especially over the lower hemisphere of spherical cavities. We also recognize that probably only experiments can definitively confirm this view. We also feel that rapid condensation on first walls and other structure that is maintained sufficiently cool, but exposed by film disruption, may also reduce the necessity for complete recoverage after every pellet microexplosion.

TABLE 1: Reynolds number (N_{Re}) dependence of turbulent flow index (n) for pipe flow.

N_{Re}	n	$\frac{(n+1)^2}{N(n+2)}$
4	6.0	1.0204
23	6.6	1.0159
110	7.0	1.0125
1100	8.8	1.0101
7000	10.0	1.0083
3200	10.0	1.0083

Table II: Equivalent sand roughnesses (e) for some pipe materials of construction.

Material	e (cm)
Polished metals	0.000
Commercial steel or wrought iron	0.005
Asphalted cast iron	0.012
Galvanized iron	0.015
Cast iron	0.026
Smooth concrete	0.030

Centrifugal Acceleration and Pressure of Film in Spherical Cavities

Neglecting gravity and second order effects due to the ange in velocity, thickness, and flow path width of the film :n distance in the direction of flow, the magnitude of the :eleration imparted to a fluid element as it is forced to low a curved path is:

$$\frac{v^2(x,\theta)}{R}$$

the pressure at any point in the film is given by:

$$P(x,\theta) = \int_x^{\delta(\theta)} \rho_L \frac{v^2(x,\theta)}{R}\, dx$$

$$= \rho_L\, \delta(\theta)\, \frac{v_m^2(\theta)}{R}\, \frac{n(N_{Re}(\theta))}{n(N_{Re}(\theta))+2} \left[1 - \left(\frac{x}{\delta(\theta)}\right)^{\frac{2}{n(N_{Re}(\theta))}+1}\right]$$

:he pressure at the free surface is taken as equal to zero ionzero pressure at the free surface is additive), where x :he distance through the film from the solid/fluid :rface. The pressure at the pipe wall $P_w(\theta)$ is therefore:

$$P_w(\theta) = \frac{n(N_{Re}(\theta))}{n(N_{Re}(\theta))+2}\, \rho_L\, \delta(\theta)\, \frac{v_M^2(\theta)}{R}$$

$$- K\rho_L\, \delta(\theta)\, \frac{\bar{v}^2(\theta)}{R} \qquad (67)$$

As an example, if $v_\ell(\theta)$, $\delta(\theta)$, R, and ρ_L are respectively 1000 cm/s, 2 cm, 2 m, 0.5 g/cm^3, and $n(N_{Re}(\theta))$ is 10, then the acceleration at the free surface is ~ 5.5 G, but $P_w(\theta)$ is only ~ 4.3×10^{-3} atm.

Nozzle Design

Although we are not yet in a position to ascertain the importance of influences of the initial velocity and pressure distribution, as determined by the injection nozzle, on such significant characteristics of liquid metal films used in modified wetted wall inertial fusion reactor cavities for protection of first walls and removal of trapped soft x-ray and pellet debris energy as uniformity, stability, ability to split the flow around beam ports, etc. However, uniform exit pressures (outside of thin boundary layers) and negligible secondary flows are probably desirable. Large discharge coefficients (ratio of mass flow rate to mass flow rate through an ideal nozzle that expands an identical working fluid from the same initial conditions to the same exit pressure) are also clearly desired for minimization of pumping power. The nozzle geometry required for injection of liquid metal films into wetted wall reactor cavities is unusual - they must be in the form of long, narrow slits - and only recently has design of such nozzles received much attention. In addition transition from a circular conduit to the planar nozzle geometry is of concern.

The four nozzle configurations depicted schematically in Figure 7 have been examined recently in a series of experiments designed to permit rating of them on the basis of uniformity of flow, turbulence intensity, total pressure loss, and discharge coefficient.[7] Table III is a summary of the resultant rankings and experimental discharge coefficient values are presented in Figure 8. Nozzle geometries A and C both appear to be superior to nozzle geometries B and D and to have acceptable characteristics. However, a few words of caution are necessary here. The experiments whose results are summarized here were performed at low Reynolds number values (for slit length the characteristic dimension, 3.4×10^3 to 2.5×10^4), whereas nozzle Reynolds number values of interest for the present application may approach 10^8. On the other hand, the experimental discharge coefficient values appear to approach asymptotically constant values as the Reynolds number increases.

A further concern is erosion and corrosion, which generally increase with increase in velocity in liquid metal flow loops, of nozzles. Periodic replacement of nozzles may be required and designs that permit inexpensive (low maintenance costs) and rapid (short downtimes, if replacement during necessary shutdown for other scheduled maintenance is not possible) replacement may be essential.

TABLE III : Rating of Nozzle Configurations

Nozzle Characteristics	Quality		
	Best	Fair	Worst
Uniformity of flow	B	A,C,D	---
Turbulence intensity	A,B,C	-----	D
Total pressure loss	B	A,C	D
Discharge coefficient	A,C	D	B

PUMPING POWER REQUIRED FOR CIRCULATION OF LIQUID METAL FOR FIRST WALL PROTECTION

The steady-flow mechanical energy equation for the external portion of the liquid metal circulation system depicted schematically in Fig. 9 can be expressed in the form:

$$\eta_p P_p = \dot{m}\eta_p w_p = \dot{m}\left[\frac{p_B}{\rho_L} + g z_B + \frac{\alpha_B \bar{v}_B^2}{2} + h_f - \frac{p_A}{\rho_L} - g z_A - \frac{\alpha_A \bar{v}_A^2}{2}\right]$$

where η_p, w_p, z, α, $\bar{v}$, h_f, and P_p are respectively the pump efficiency (for conversion of electrical power input into flow energy), actual pump work per unit mass, height above a horizontal reference plane, velocity factor (ratio of v^2 to $\bar{v}^2$), local average velocity of the flowing liquid, conversion of flow energy into internal energy by viscous forces (friction loss) per unit mass flowing through the external portion of the circuit, and the actual pumping power requirement and the subscripts A, B, and C denote the indicated stations around the flow loop. The station C is located at the vena contracta of the injection nozzle.

The friction loss in the external portion of the flow loop can be broken up into a variety of terms:

$$h_F = \sum 4 f_p \frac{L_p}{D_p} \frac{\bar{v}_p^2}{2} + \sum K_B \frac{v_B^2}{2} + \sum K_{CE} \frac{\bar{v}_{CE}^2}{2} + \sum K_{FV} \frac{\bar{v}_{FV}^2}{2} + \sum K_{HX} \frac{\bar{v}_{HX}^2}{2} \qquad (64)$$

where L and D are pipe length and diameter, K is a so-called resistance coefficient, and the subscripts P, B, CE, FV, and HX refer respectively to pipes, bends, contractions and expansions, valves and other fittings and the heat exchangers. Typical values of K_p are ~ 0.85.

The velocity in the vena contracta of the injection nozzle can be related to the presure drop across the nozzle according to:

$$\bar{v}_C = \frac{\sqrt{\frac{2}{\rho_L}\left[g_L g(z_B - z_C) + (P_B - P_C) + \alpha_B \rho_L \bar{v}_B^2\right]}}{\sqrt{\alpha_C + K_N}}$$

where K_N is the resistance coefficient of the nozzle. This relation results from a mechanical energy balance across the nozzle of the same type as that for the external part of the flow loop. Because $A_C << A_B$, so that $v_B << v_C$, stations B and C are close together (so that $z_B \sim z_C$), and K_C must be very low, the preceding equation becomes:

$$\bar{v}_C = \frac{\sqrt{2P_B/\rho_L}}{\sqrt{\alpha_C + K_N}} = C_D\sqrt{2P_B/\rho_L}$$

where C_D is the discharge coefficient (maximum value ~ 0.9) discussed in the preceding section. Also:

$$v_C = \bar{v}(\theta_0)$$

so that:

$$P_B \sim \frac{\rho_L}{2}\left[\frac{\bar{v}(\theta_0)}{C_D}\right]^2 \qquad (7)$$

We further simplify our analysis by introducing a number of additional assumptions and approximations:

- The external portion of the liquid metal circuit is generously sized so that the friction loss per unit mass in this portion of the flow loop can be neglected.

- The velocity at stations A and B are either low enough to be neglected or differ negligibly.
- The nozzle outlet corresponds to its vena contracta.
- Neglect of variations in liquid properties around the flow loop will not introduce significant error.

In addition P_A must be very small. These assumptions and approximations allow us to write:

$$\eta_p P_p \sim \dot{m} \frac{P_B}{\rho_L} + g (z_B - z_A) \qquad (\ )$$

Then we let:

$$z_B - z_A = 2R + H \qquad (\ )$$

where H is large enough to accommodate a blanket and necessary room for pumps, pipe bends, etc. Combination of these results with Eq. 75 results in:

$$P_p \sim \frac{\dot{m}}{\eta_p} \left[\frac{1}{2} \frac{\bar{v}(\theta_0)}{C_D} \right]^2 + g (2R + H) \qquad (\ )$$

We also recall that:

$$\dot{m} = 2\pi R \sin(\theta_0)\, \delta(\theta_0)\, \bar{v}(\theta_0) \rho_L \qquad (77)$$

we see that the effects of increasing ρ_L on P_p are minimized by minimizing R and H and that reducing $\dot{m}$ reduces P_p. Both $(N_p)'$ and C_D are, for practical purposes, fixed.

As an example, if we use lithium as the protective liquid metal (ρ_L = 0.494 g/cm^3), use the recommended values for C_D (0.9) and $(N_p)'$ (0.85), and let θ_0, $\delta(\theta_0)$, $\bar{v}(\theta_0)$, R and H be respectively 15°, 2 cm, 20 m/s, 2 m, and 6 m (giving $\dot{V}$ = 1.30 m^3/s and $\dot{m}$ = 643 kg/s), we obtain P_p = 0.261 Mwe. By way of comparison, the above parameter values might correspond to a 5-hertz reactor with 150-MJ yield pellets whose gross thermal power is at least 750 MWt. The corresponding electric power output would typically exceed 250 Mwe. Furthermore, if the required increase in $v(\theta_0)$ with increase in pellet yield, and hence with R, is not excessive, then because R increases approximately as $Y^{1/2}$ a similar ratio of power consumption for liquid metal circulation to power prodiction per cavity would be representative. Power consumption becomes a more significant concern if the use of much high atomic number liquid metals is contemplated, for not only are they generally considerably more dense, but also typically have substantially lower specific heat capacites so that circulation at a much greater mass rate for the same duty may be necessary. By way of example, if the protective liquid metal were Li_2Pb_7 and the allowable temperature rise remained the same, we would have ρ_L = 10.5 g/cm^3 instead of = 0.5 g/cm^3 and c_L = 0.155 J/gK instead of = 4.2 J/gK, so that $\dot{m}$ would have to be = 570 times as great if the circulation rate were determined by thermal transport considerations alone with no transfer through walls. However, the flow rate assumed above for lithium is almost four times that required for thermal energy transport. Also, because of much higher density, the required volume flow rate increase is less and pressure drops through nozzles depend on volume flow rate squared rather than mass flow rate and on density only to the first power.

Protection of Injection Nozzles, Splitting of Flow Around Beam Ports, Etc.

The injection nozzles (and any other equipment that must protrude into wetted-wall reactor cavities) must be protected from pellet soft x ray and debris ion emissions. In addition, the protective liquid metal film must be pierced by openings for passage of driver beams and some first wall structure requiring protection could be exposed in forming these openings. ~~The latter set of design problems is common to all fluid wall inertial fusion reactor concepts.~~ We do have some ideas for protection of injection nozzles. Assured protection of small areas by controlled seepage of liquid metal through porous walls is believed to be easier than similar protection of large areas. Thick sacrificial shields could be used over small areas and these small areas could be designed for convenient periodic changeout.

The types of liquid metal films under consideration for first wall protection in modified wetted-wall reactor concepts apparently will place some restrictions on location of driver beam parts or at least make design for arbitrary placement more difficult. A substantial degree of uniformity of illumination may be required for commercial applications pellets, although this has not yet been established and current trends are away from uniformity. On the other hand, sheer bulk of beam transport and final focusing equipment for some drivers may force spreading out of beam ports. This ~~situation is common to all fluid-wall inertial fusion reactor concepts~~. If complete reformation of protective films after each pellet microexplosion is necessary and cavity sizes are such that this cannot be accomplished by injection nozzles at only one location, the use of multiple slit injection nozzles may make design for relatively uniform illumination easier. If beam ports can be clustered in a vertical linear array extending from reactor top to reactor bottom, then simple raised lips, which will, however, require some protection, can be used to keep film liquid ~~injected for protection of other reactor first wall areas~~ from intruding into beam tubes. If only a single location for protective film injection at the top of a reactor cavity is

provided and diversion around beam ports is required, raised lips and auxiliary vanes (which can perhaps be submerged) are suggested for splitting and rejoining of the films.

The solutions suggested above to the perceived problems of nozzle protection and provision for driver pulsed energy injection are clearly only conceptual in nature. ~~However, these proposed solutions are similar in kind and degree of development to solutions to the same class of design problems for other fluid wall inertial fusion reactor concepts that have been advanced.~~ Nonetheless, considerably more study of these problems will ~~probably~~ be required.

Closure

A modification of the original wetted-wall inertial fusion rector concept for commercial applications (in which restoration of cavity atmosphere conditions following pellet microexplosions to those required for driver energy pulse transmission to targets with acceptable degradation is accomplished by exhaust of vaporized liquid metal used for cavity first wall protection through a nozzle and the liquid metal films are formed by forcing the liquid metal through a porous first wall) has been described. The modification (in which cavity atmosphere restoration is accomplished through condensation and first wall coverage by injection through slit nozzles) offers a number of potential advantages when compared to the original wetted-wall concept, including:

* assured reactor cavity first wall protection;

  higher reactor pulse repetition rates;

* separation of blanket and first wall protection functions;

* replacement of a supersonic nozzle and condenser by a simple drain; and

* adaptability for use with heavy-ion drivers.

A number of the topics that must be considered in establishing the technical and economic viability of our modified wetted-wall concept have been addressed with favorable results. These include:

* cavity clearing times;

* pumping power requirements;

* first wall recoverage time;

* film thicknesses;

* protection of exposed structure and diversion around beam ports;

* film stability;

* thermal energy transport requirements;

* neutron kinetic and interaction energy deposition in the films; and

* centrifugal forces acting to keep the films on cavity walls.

However, there are additional questions, some common to all fluid-wall inertial fusion reactor concepts and others peculiar to our new concept, that must be answered if viability of the new concept is to be confirmed. For example, we must develop:

* theory or experiments to characterize possible film fragmentation and

* aerosol formation;

* a method for specifying the extent of first wall recoverage required after each pellet microexplosion;

* experiments or more accurate theoretical methods for determination of cavity clearing times;

* solutions to potential corrosion/erosion problems;

* designs for protection of exposed structure and diversion of films around beam ports;

* theory or experiments to better characterize the energy partition; and

* the tools to examine various aspects of reactor/driver interfaces, pellet injection and tracking, etc.

in modified wetted-wall reactors. The required degree of uniformity of pellet illumination also needs to be definitively established.

We have not yet begun the difficult optimization process that would lead to selection of a protective liquid metal and ~~values for, e.g., $\bar{\gamma}(a_0)$, and $\sigma(a_0)$, a_0, k, γ, aI_A,~~ that would result in the minimum cost of, say, production of electric power using inertial fusion energy sources. The optimum set of ~~parameter values~~ operating conditions, will, in general, be different for different drivers, energy conversion cycles, etc., and ~~the set of values considered optimum~~ will undoubtedly change substantially as our level of understanding of modified wetted-wall cavity phenomenology increases. The effects of changes in ~~value for the parameters~~ operating conditions will extend throughout a fusion power plant and therefore a major systems study will be required for optimization.

References

1. L. A. Booth (Compiler), "Central Station Power Generation by Laser-Driven Fusion," Los Alamos Scientific Laboratory report LA-4858-MS, Vol. 1 (February 1972).

2. L. A. Booth and T. G. Frank (Compilers), "Commercial Applications of Inertial Confinement Fusion," Los Alamos Scientific laboratory report LA-6838-MS (May 1977).

3. W. M. Rohsenow and J. P. Hartnett (Editors), Handbook of Heat Transfer, W. M. Rohsenow, "Condensation, Part A," McGraw-Hook Co., New York, 1973, Section 12.

4.

5.

6. J. H. Vennard, "One-Dimensional Flow," Handbook of Fluid Dynamics (V. L. Streeter, Editor), First Edition, McGraw-Hill Book Co., Inc., New York, 1961, Section 3.

7. J. A. Owczarek and D. O. Rockwell, "An Experimental Study of Flows in Planar Nozzles," Journal of Basic Engineering, Trans. ASME, Series D, 94, 682, (1972).

8. [redacted]

Fig. 1. Schematic of modified wetted-wall inertial fusion commercial applications reactor concept.

Fig. 4. Li_1 and Li_2 partial pressures and corresponding equilibrium vapor lithium atom density.

Fig. 2. Effect of variation of parameter values one at a time about a reference set of values on the cavity clearing time for clearing by exhaust through a nozzle.

Fig. 3. Effect of variation of parameter values one at a time about a reference set of values on the cavity clearing time for clearing by condensation.

Fig. 5. Schematic of simplified film flow model.

Fig. 6. Film thickness, reformation time, and average velocity as functions of angular position for various initial film thicknesses with $\theta_0 = 15^0$, $v(\theta_0) = 20$ m/s, $e = 0.002$, $R = 2$ m, and $\eta_L = 0.007895$ cm^2/s.

Fig. 6b. Film thickness, reformation time, and average velocity as functions of angular position for various initial film thicknesses with $\theta_0 = 15^0$, $v(\theta_0) = 50$ m/s, $e = 0.002$, $R = 2$ m, and $\eta_L = 0.007895$ cm^2/s.

Fig. 6c. Film thickness, reformation time, and average velocity as functions of angular position for various initial film thicknesses with $\theta_0 = 15^0$, $v(\theta_0) = 100$ m/s, $e = 0.002$, $R = 2$ m, and $\eta_L = 0.007895$ cm^2/s.

Fig. 7. Nozzle geometries whose characteristics have been investigated experimentally.

Fig. 8. Experimental discharge coefficients as a function of Reynolds number.

Fig. 9. Schematic of liquid metal flow loop.

Captions for Fig. 6d
6e
6f
6g

FIG. 1: MODIFIED WETTED WALL REACTOR

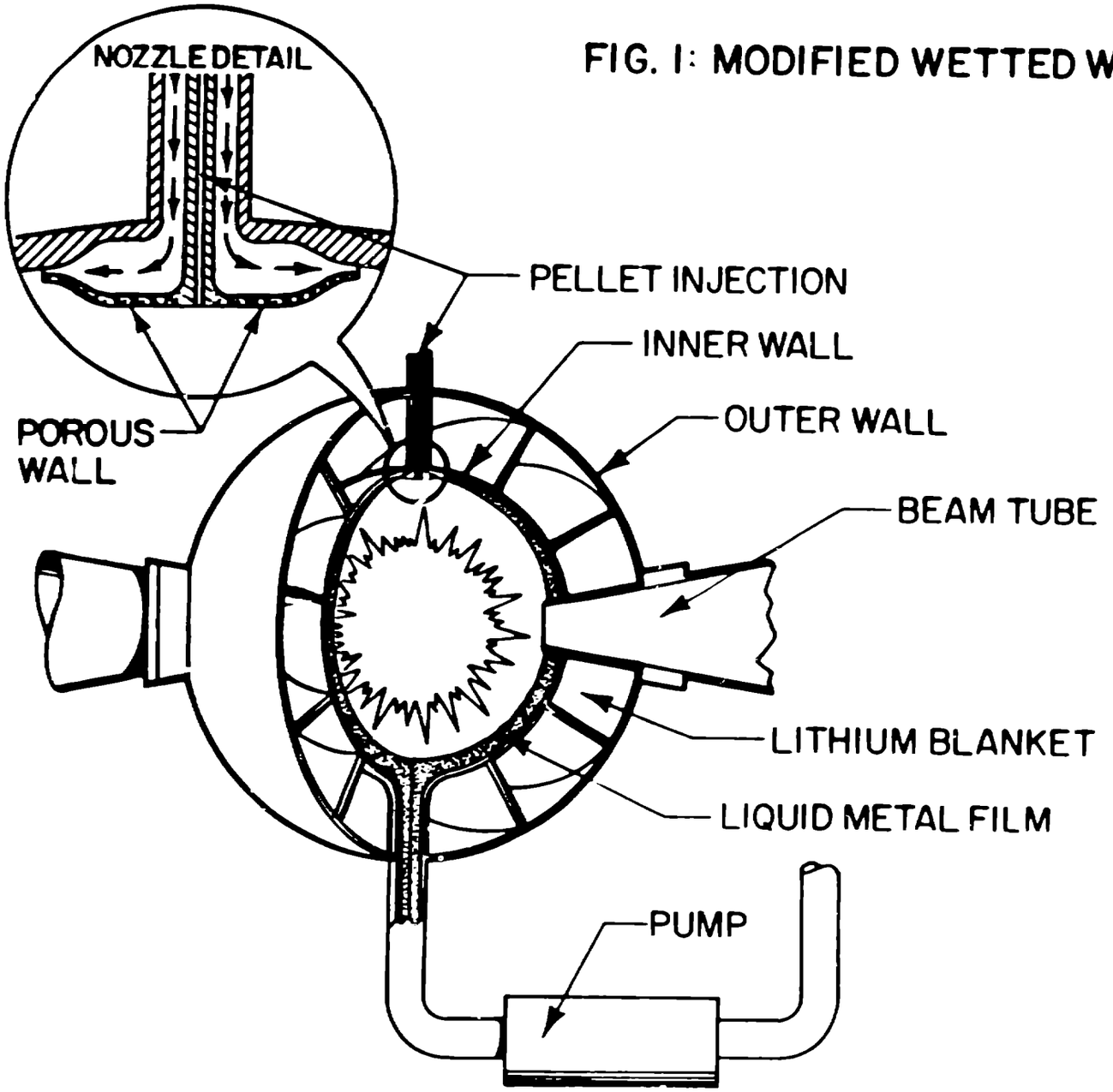

Fig. 2

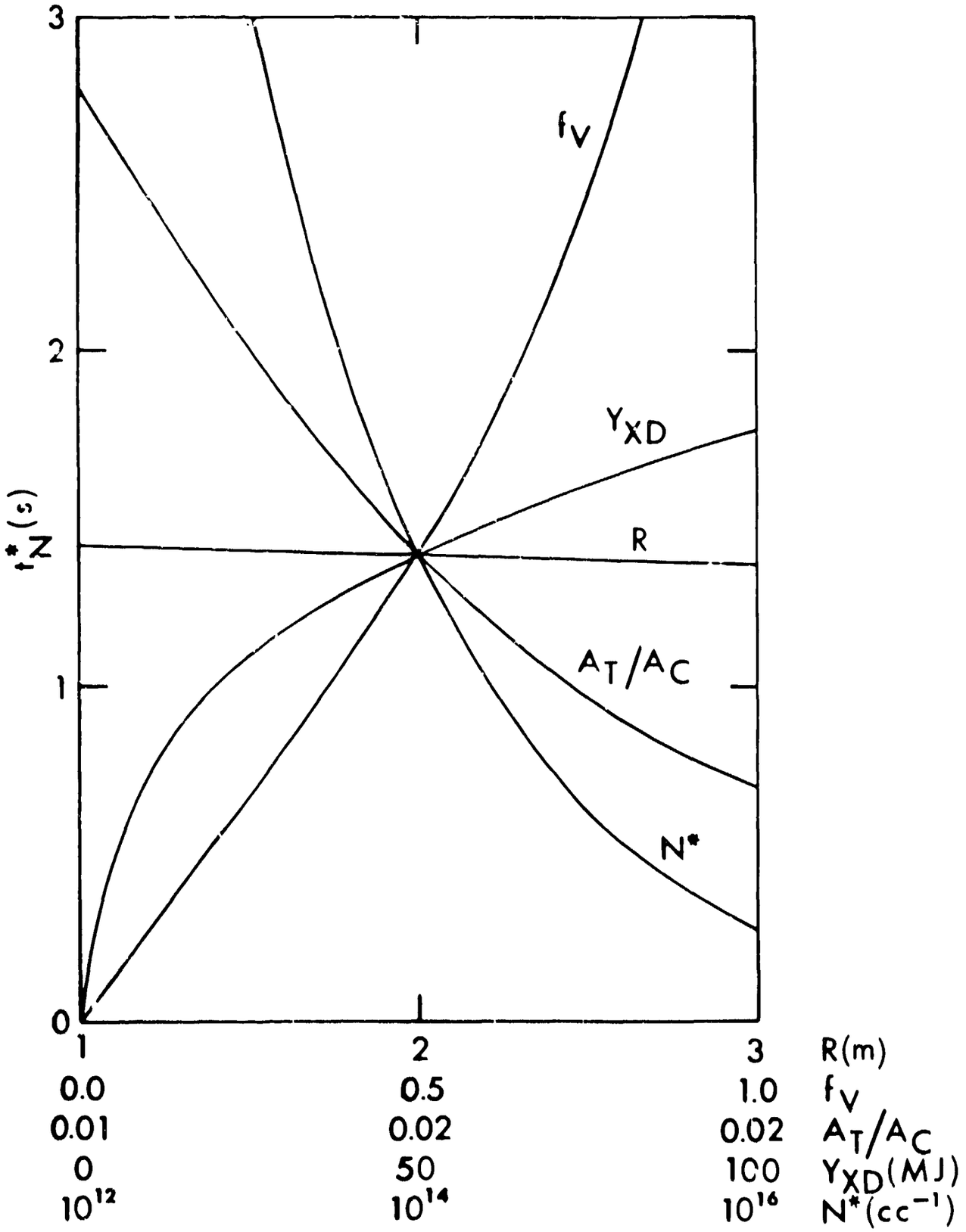
3
2
1
0
f_V
Y_{XD}
R
A_T/A_C
N^*
$t^*_{\downarrow Z}$ (s)
1
2
3
R(m)
0.0
0.5
1.0
f_V
0.01
0.02
0.02
A_T/A_C
0
50
100
Y_{XD}(MJ)
10^{12}
10^{14}
10^{16}
$N^*(cc^{-1})$

Fig 3

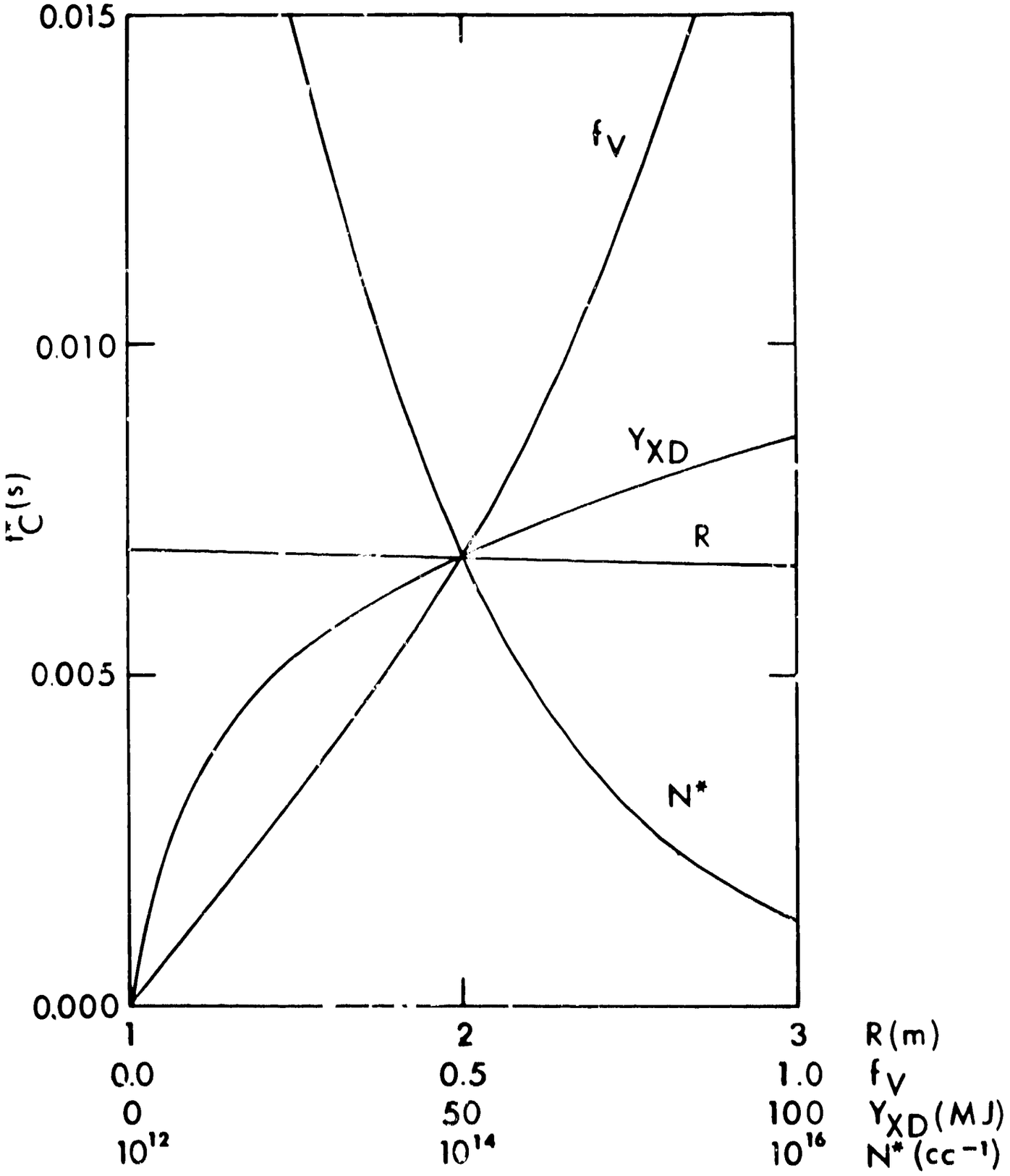
0.015
0.010
0.005
0.000
τ_C(s)
f_V
Y_{XD}
R
N*
1
2
3
R(m)
0.0
0.5
1.0
f_V
0
50
100
Y_{XD}(MJ)
10^{12}
10^{14}
10^{16}
N* (cc^{-1})

Fig. 4

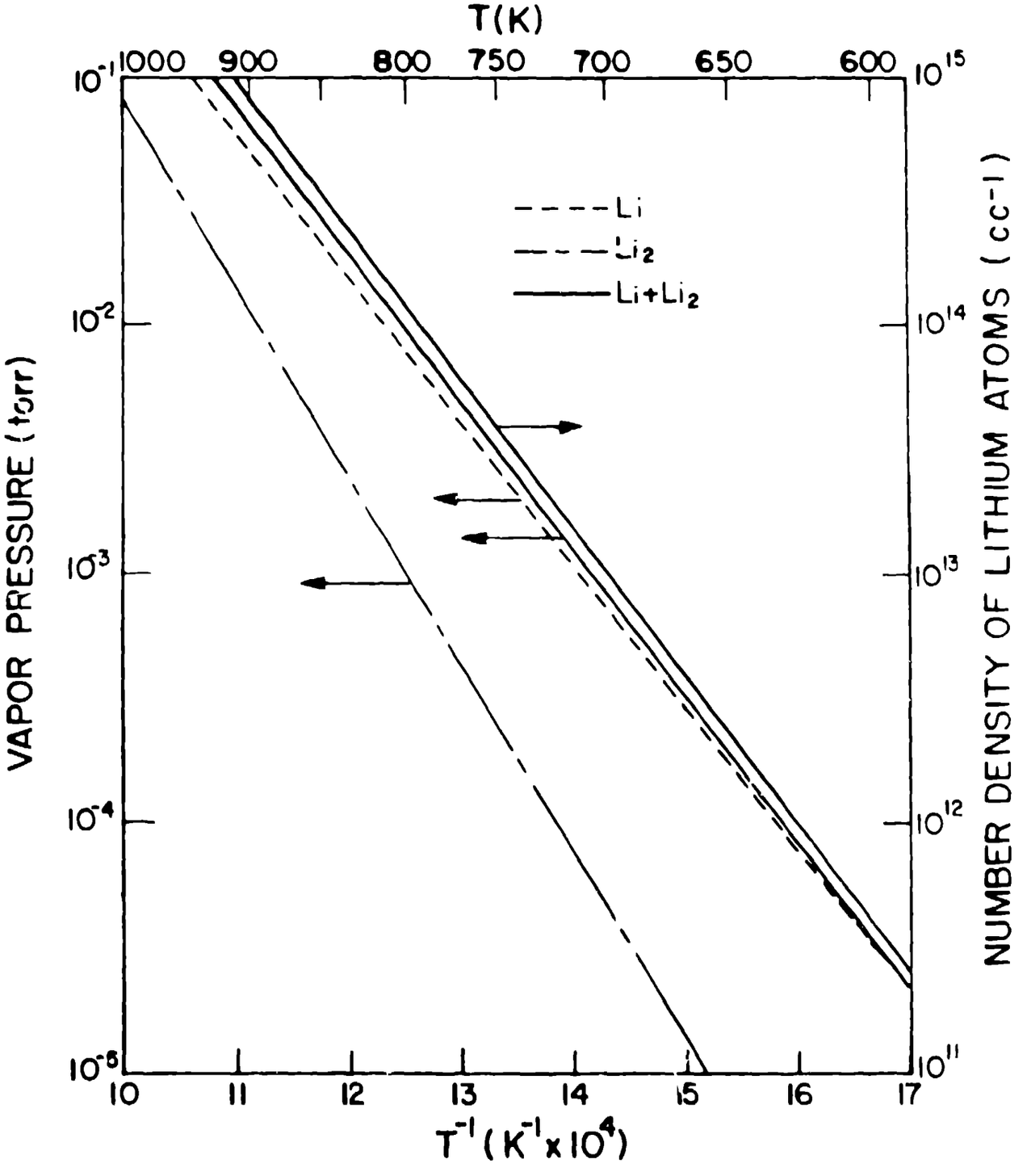
T(K)
1000
900
800
750
700
650
600
10^{-1}
10^{-2}
10^{-3}
10^{-4}
10^{-5}
10^{15}
10^{14}
10^{13}
10^{12}
10^{11}
Li
Li_2
$Li+Li_2$
VAPOR PRESSURE (torr)
NUMBER DENSITY OF LITHIUM ATOMS (cc^{-1})
10
11
12
13
14
15
16
17
T^{-1} ($K^{-1} \times 10^4$)

Fig. 5

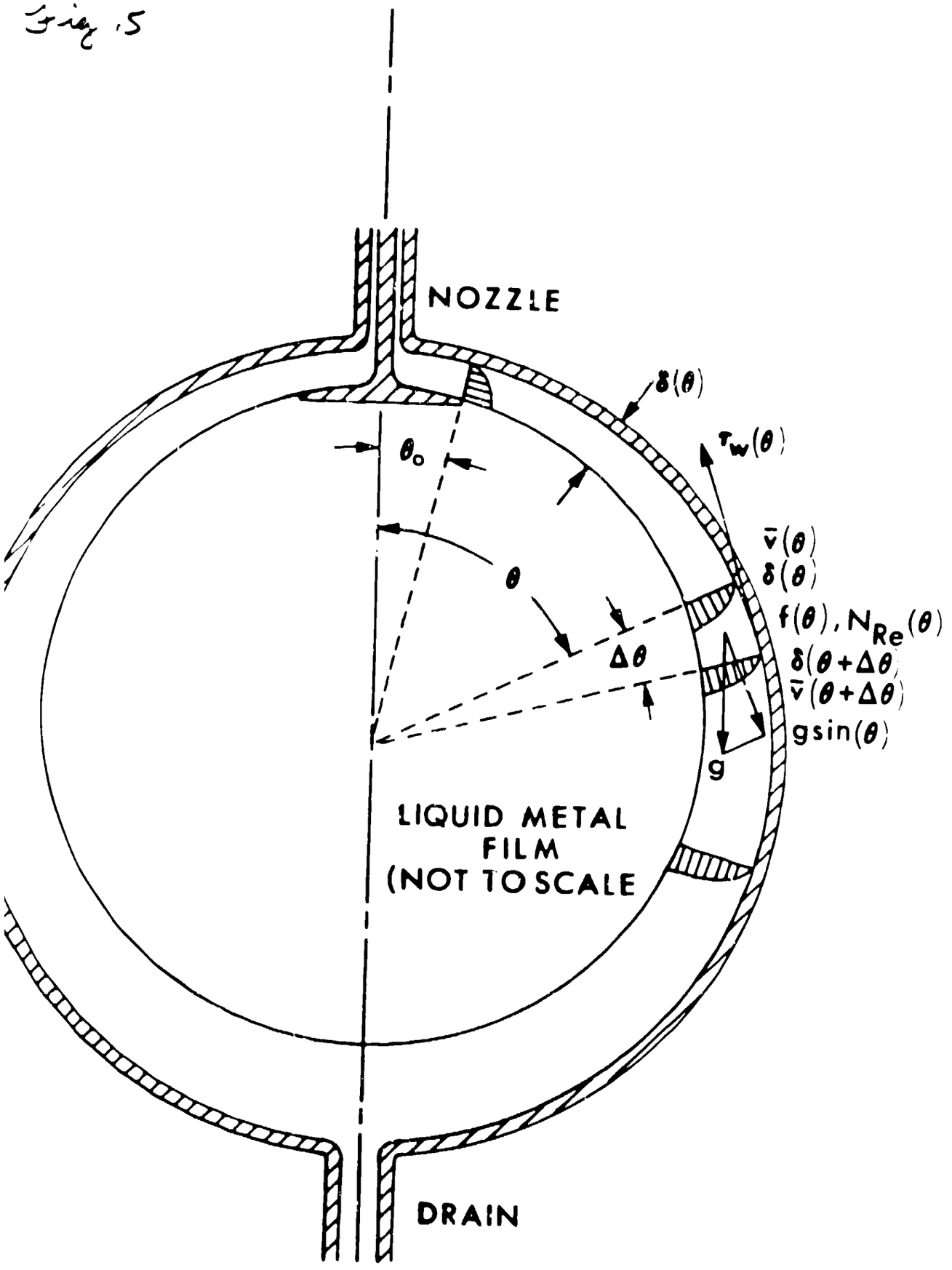
NOZZLE
$\delta(\theta)$
$\tau_w(\theta)$
θ_o
$\bar{v}(\theta)$
$\delta(\theta)$
θ
$f(\theta), N_{Re}(\theta)$
$\Delta\theta$
$\delta(\theta+\Delta\theta)$
$\bar{v}(\theta+\Delta\theta)$
$g\sin(\theta)$
g
LIQUID METAL
FILM
(NOT TO SCALE
DRAIN

Fig. 6A

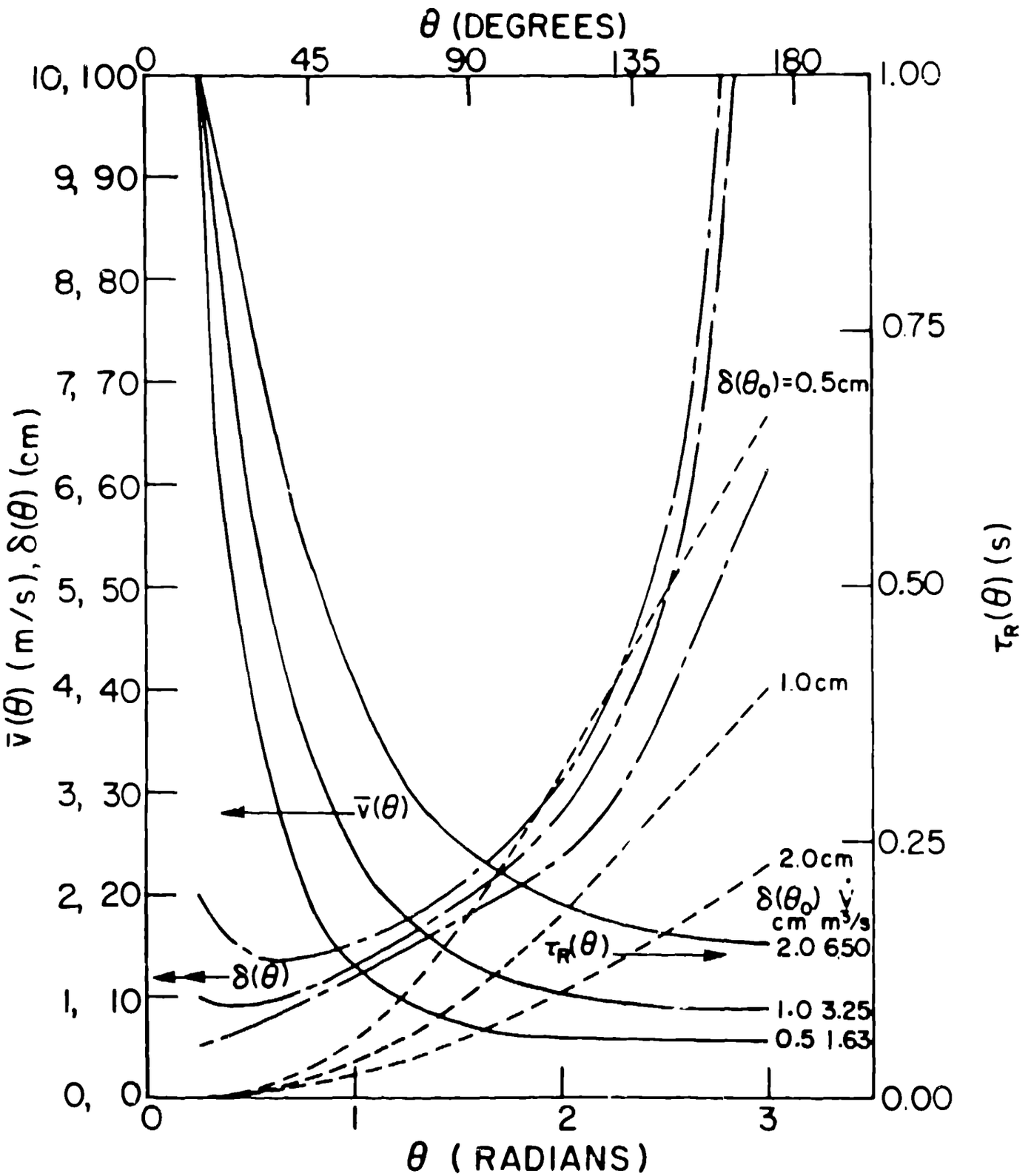
θ (DEGREES)
0
45
90
135
180
10, 100
9, 90
8, 80
7, 70
6, 60
5, 50
4, 40
3, 30
2, 20
1, 10
0, 0
1.00
0.75
0.50
0.25
0.00
v̄(θ) (m/s), δ(θ) (cm)
τR(θ) (s)
δ(θ0)=0.5cm
1.0cm
2.0cm
v̄(θ)
δ(θ)
τR(θ)
δ(θ0) cm
v̇ m3/s
2.0 6.50
1.0 3.25
0.5 1.63
0
1
2
3
θ (RADIANS)

Fig. 6B

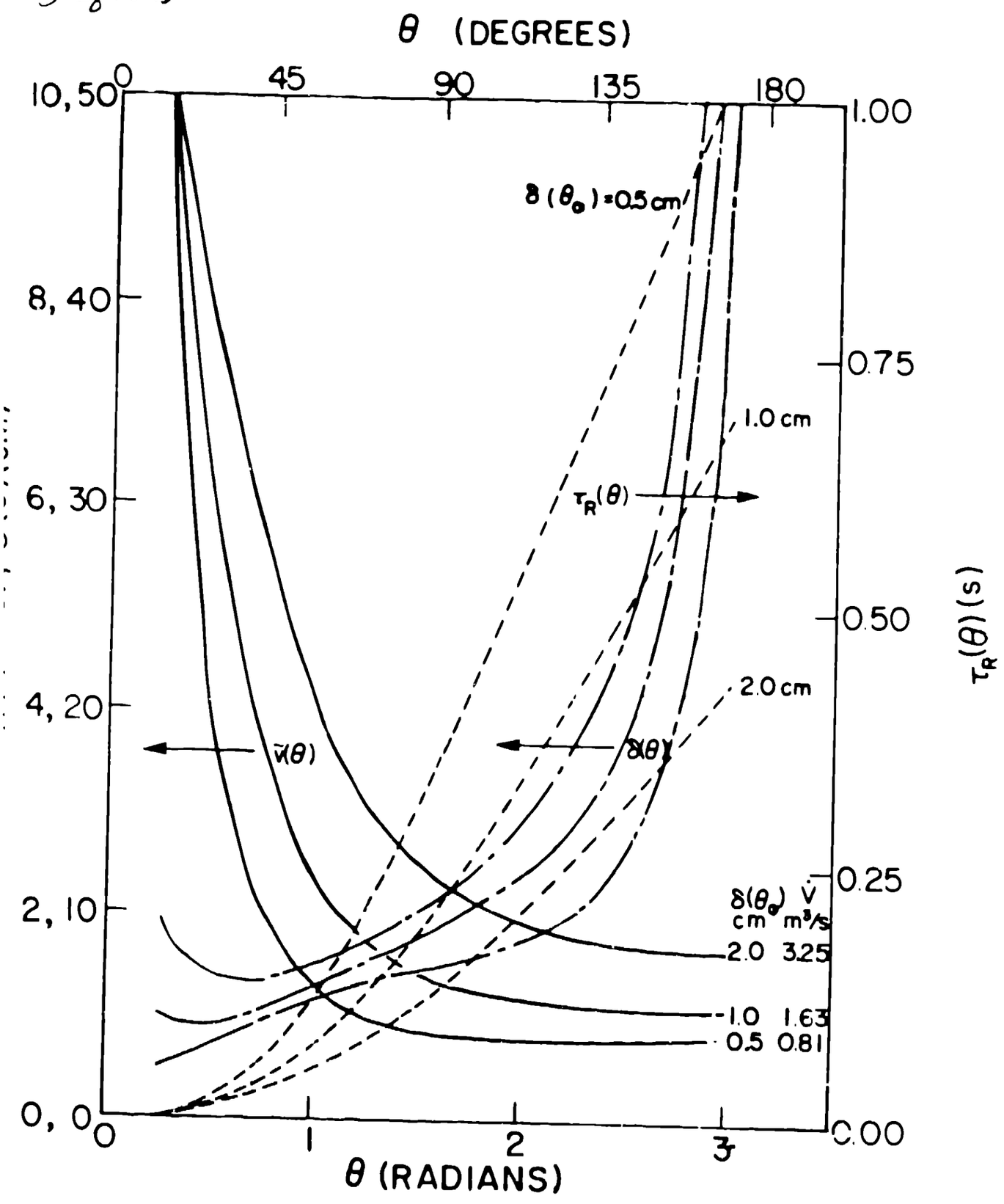
θ (DEGREES)
0
45
90
135
180
10,50
8,40
6,30
4,20
2,10
0,0
1.00
0.75
0.50
0.25
0.00
δ(θ₀)=0.5cm
1.0 cm
2.0 cm
τR(θ)
ṽ(θ)
δ(θ)
τR(θ) (s)
δ(θ₀) cm
V̇ m³/s
2.0 3.25
1.0 1.63
0.5 0.81
0
1
2
3
θ (RADIANS)

Fig. 6C

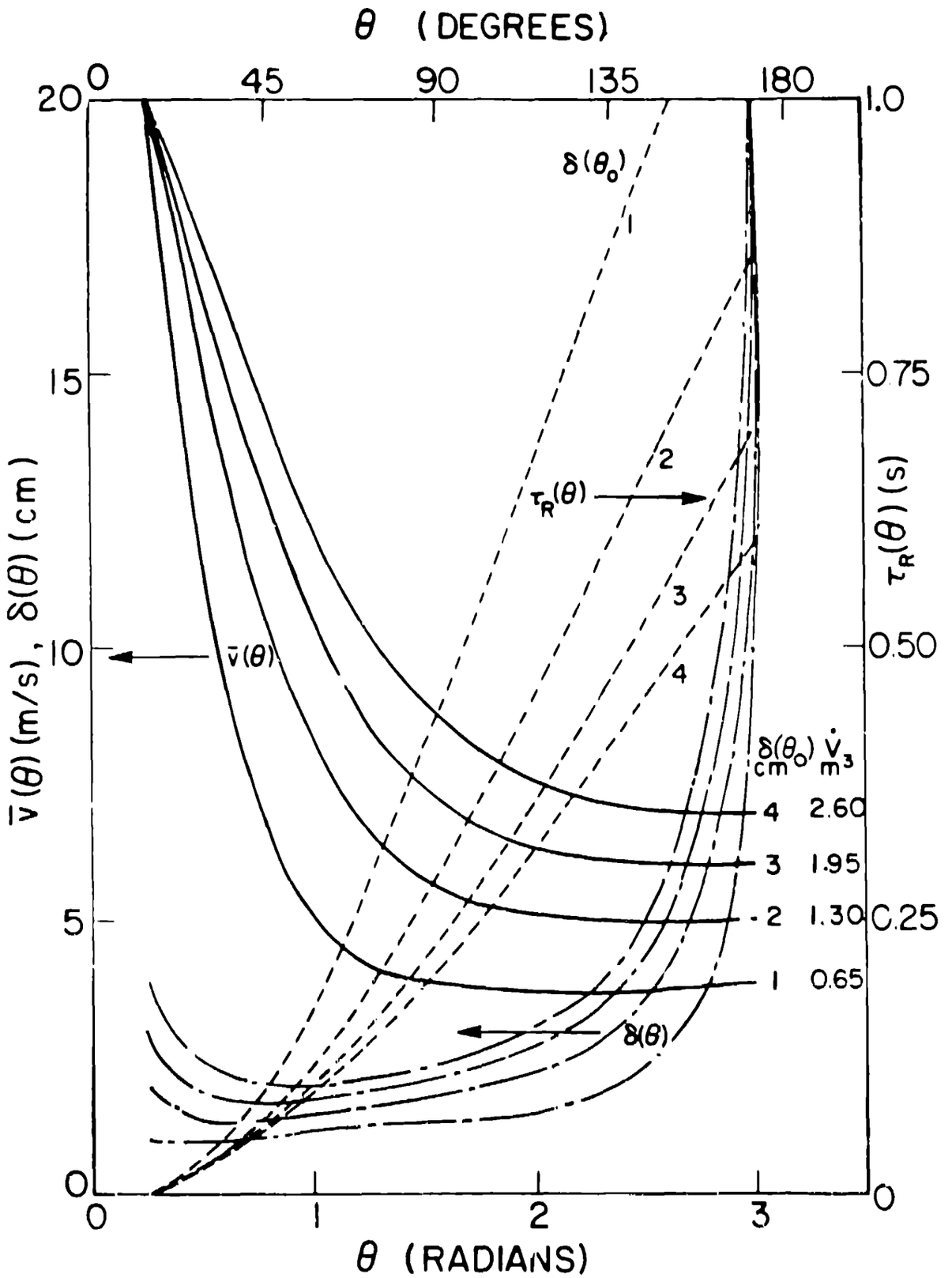
θ (DEGREES)
0
45
90
135
180
20
15
10
5
0
1.0
0.75
0.50
0.25
0
δ(θ₀)
1
2
3
4
τR(θ)
v̄(θ)
δ(θ)
v̄(θ) (m/s), δ(θ) (cm)
τR(θ) (s)
δ(θ₀) cm
V̇3 m3
4 2.60
3 1.95
2 1.30
1 0.65
0
1
2
3
θ (RADIANS)

Fig. 6D

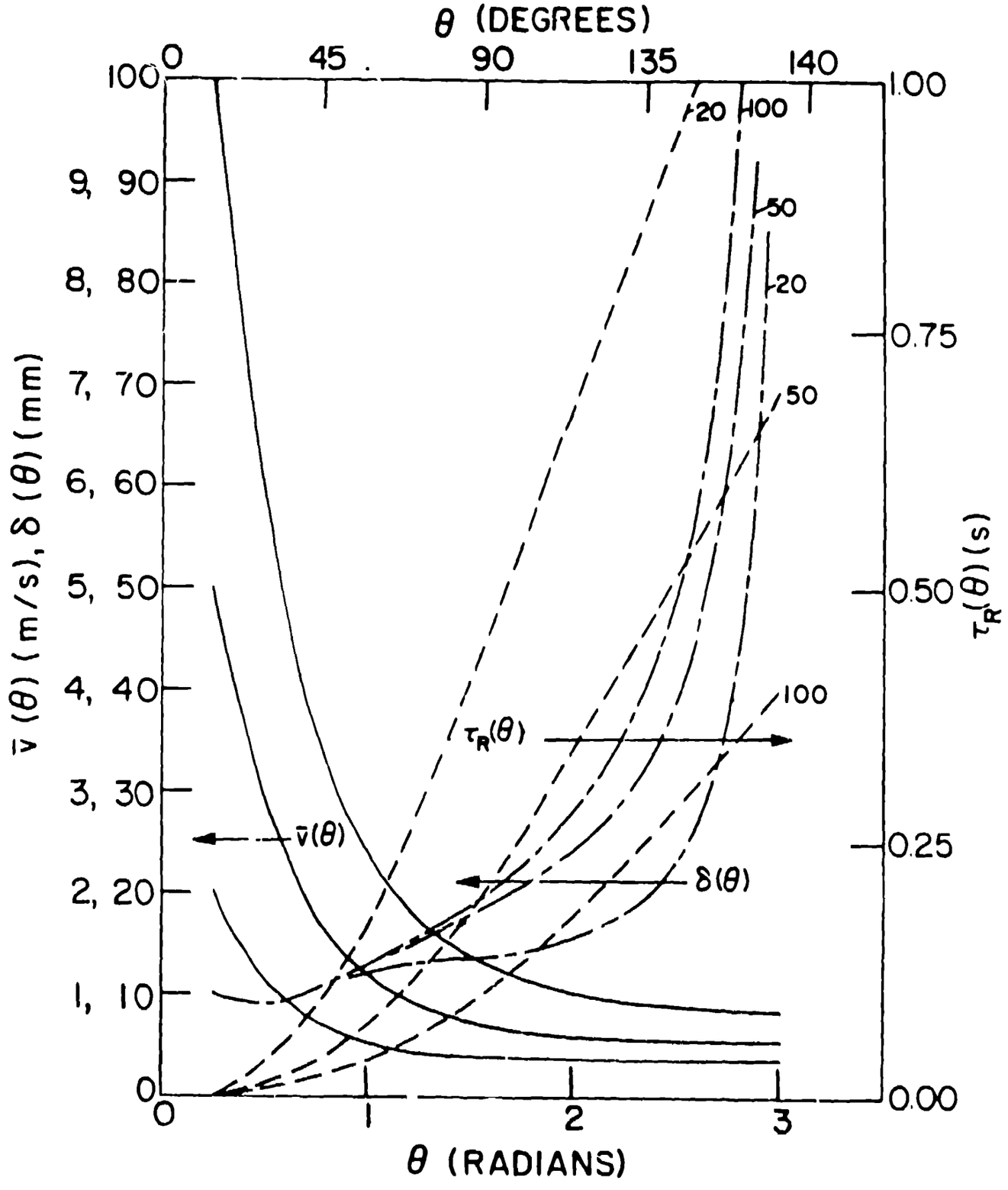
θ (DEGREES)
0
45
90
135
140
100
9, 90
8, 80
7, 70
6, 60
5, 50
4, 40
3, 30
2, 20
1, 10
0
1.00
0.75
0.50
0.25
0.00
20
100
50
20
50
100
$\tau_R(\theta)$
$\bar{v}(\theta)$
$\delta(\theta)$
$\bar{v}(\theta)$ (m/s), $\delta(\theta)$ (mm)
$\tau_R(\theta)$ (s)
0
1
2
3
θ (RADIANS)

Fig. 6E

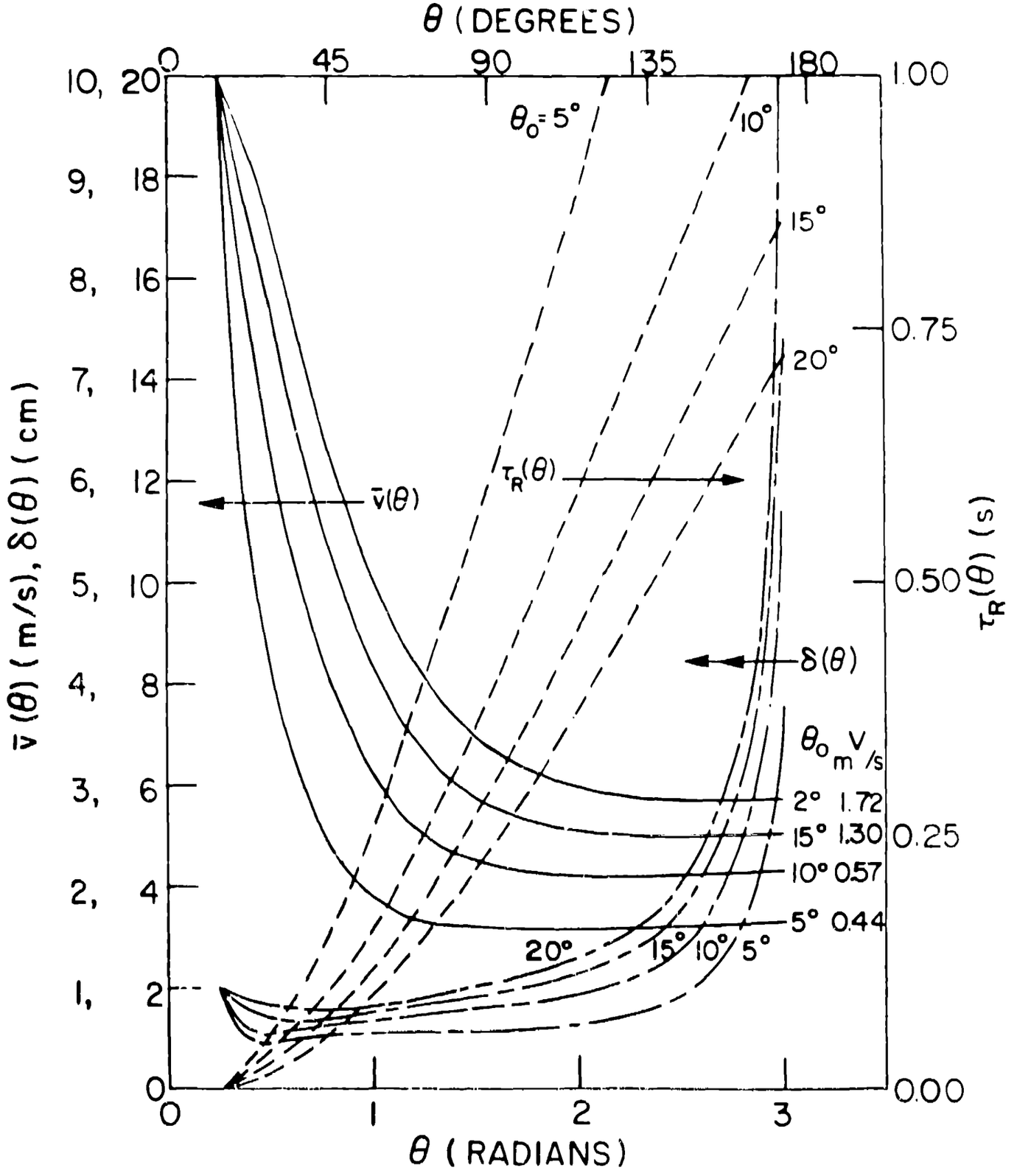
θ (DEGREES)
0
45
90
135
180
θ (RADIANS)
0
1
2
3
$\bar{v}(\theta)$ (m/s), $\delta(\theta)$ (cm)
10, 20
9, 18
8, 16
7, 14
6, 12
5, 10
4, 8
3, 6
2, 4
1, 2
0
$\tau_R(\theta)$ (s)
1.00
0.75
0.50
0.25
0.00
$\theta_0 = 5°$
10°
15°
20°
$\bar{v}(\theta)$
$\tau_R(\theta)$
$\delta(\theta)$
θ_0 m/s
2° 1.72
15° 1.30
10° 0.57
5° 0.44
20°
15°
10°
5°

Fig. 6F

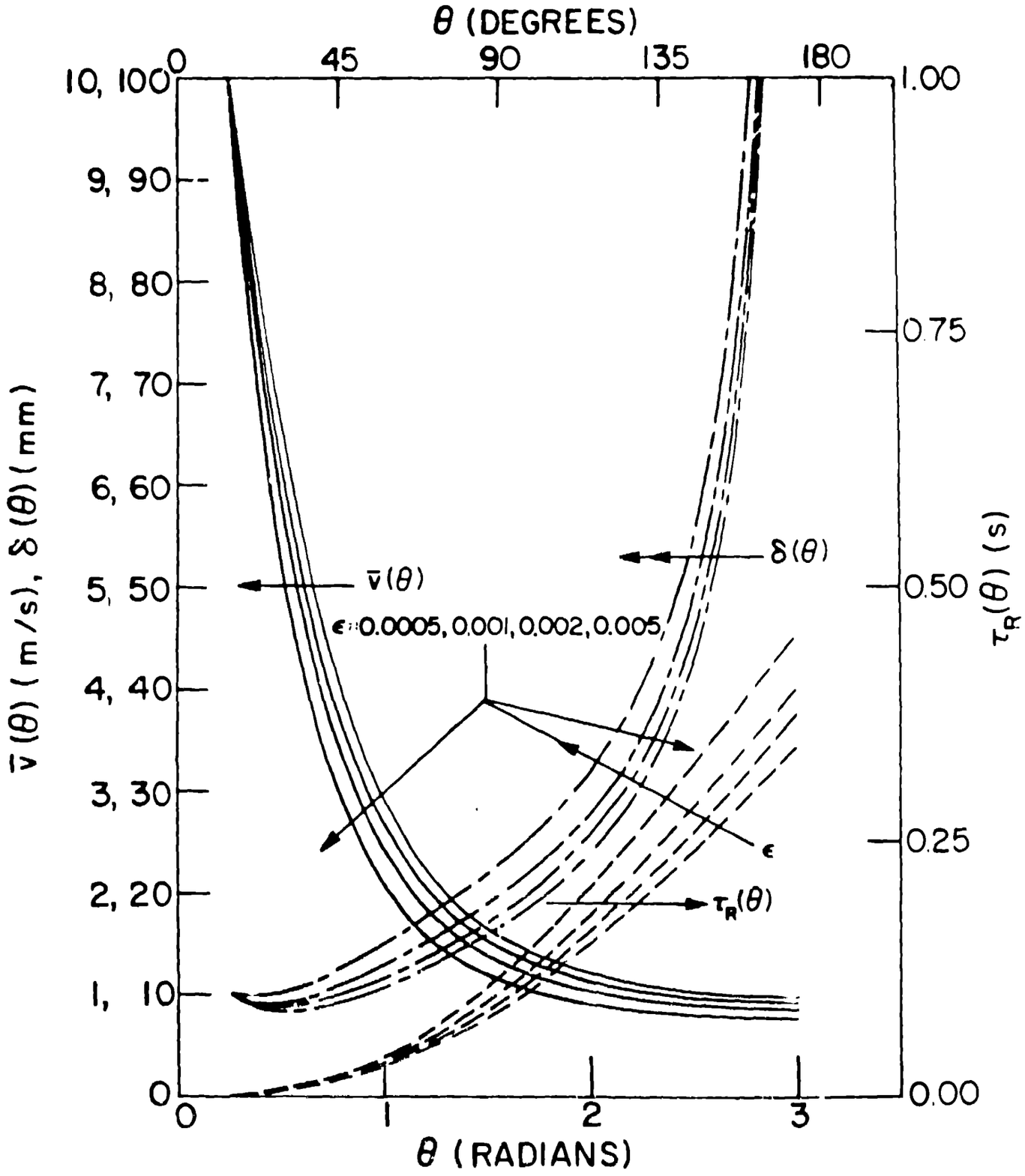
θ (DEGREES)
0
45
90
135
180
10, 100
9, 90
8, 80
7, 70
6, 60
5, 50
4, 40
3, 30
2, 20
1, 10
0
1.00
0.75
0.50
0.25
0.00
$\bar{v}(\theta)$ (m/s), $\delta(\theta)$ (mm)
$\tau_R(\theta)$ (s)
$\bar{v}(\theta)$
$\delta(\theta)$
ϵ: 0.0005, 0.001, 0.002, 0.005
ϵ
$\tau_R(\theta)$
0
1
2
3
θ (RADIANS)

fig. 6 G

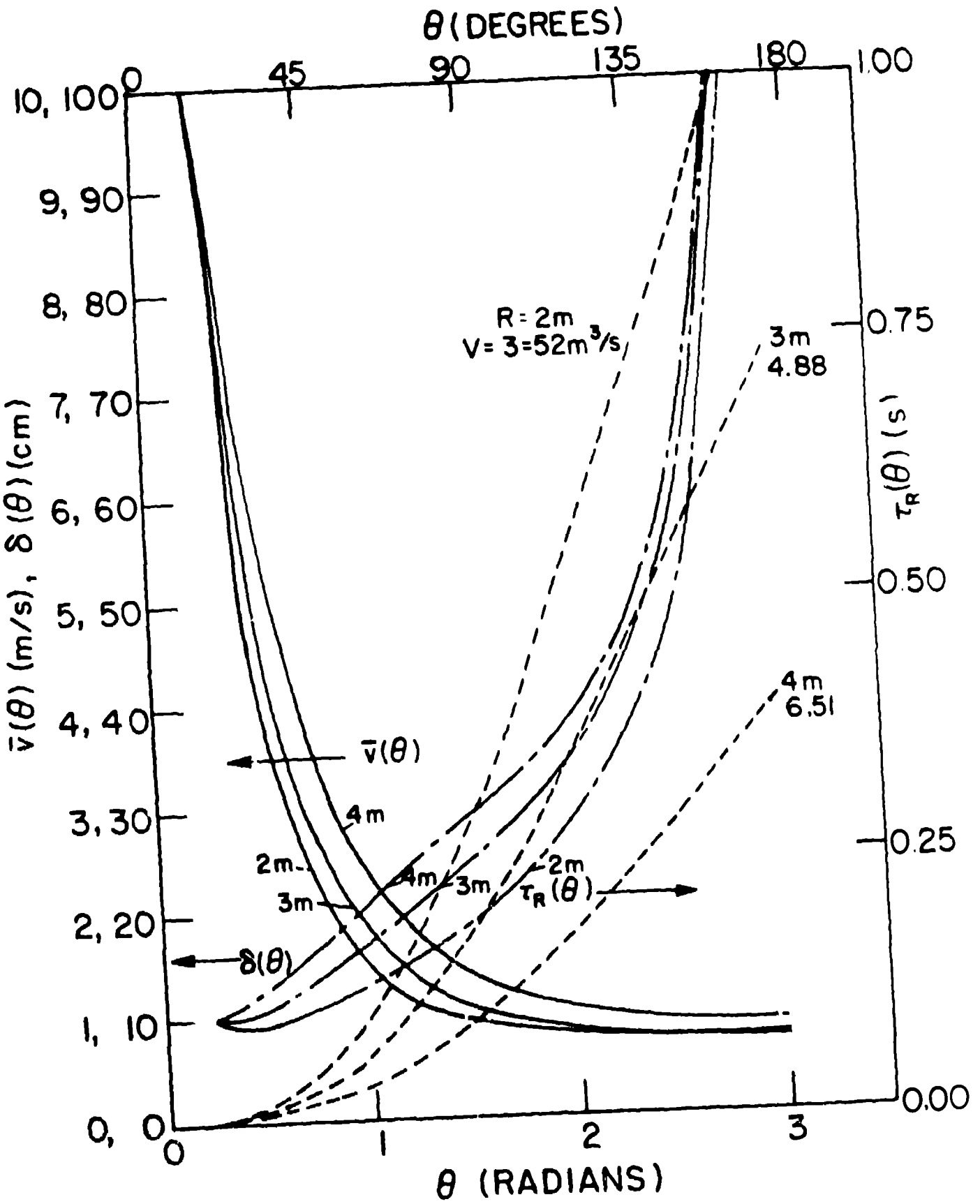
θ (DEGREES)
0
45
90
135
180
10, 100
9, 90
8, 80
7, 70
6, 60
5, 50
4, 40
3, 30
2, 20
1, 10
0, 0
1.00
0.75
0.50
0.25
0.00
v̄(θ) (m/s), δ(θ) (cm)
τR(θ) (s)
R = 2m
V = 3=52m³/s
3m
4.88
4m
6.51
v̄(θ)
4m
2m
3m
δ(θ)
4m
3m
2m
τR(θ)
0
1
2
3
θ (RADIANS)

Fig. 7

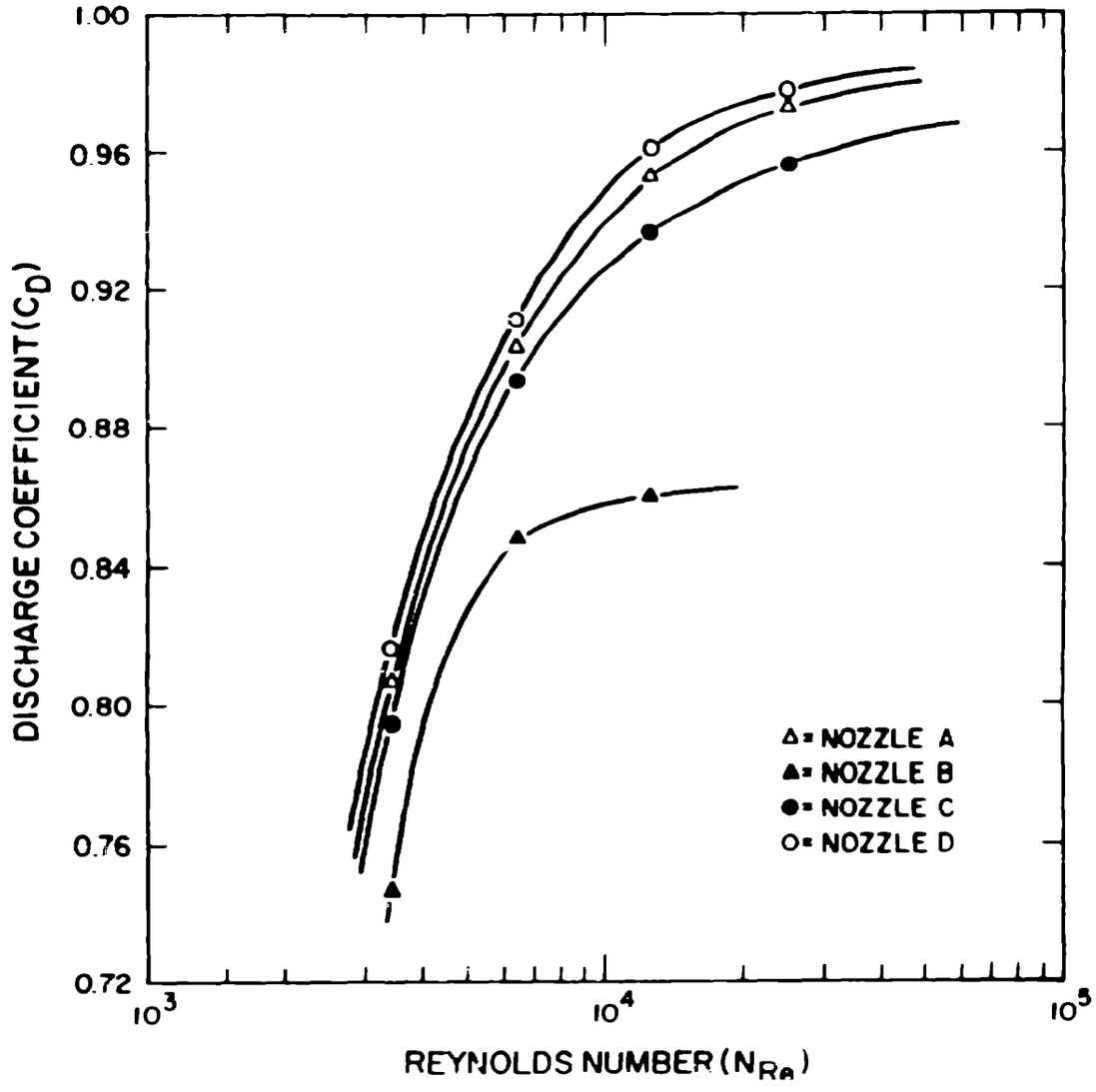
1.00
0.96
0.92
0.88
0.84
0.80
0.76
0.72
DISCHARGE COEFFICIENT (C_D)
10^3
10^4
10^5
REYNOLDS NUMBER (N_{Re})
Δ= NOZZLE A
▲= NOZZLE B
●= NOZZLE C
○= NOZZLE D

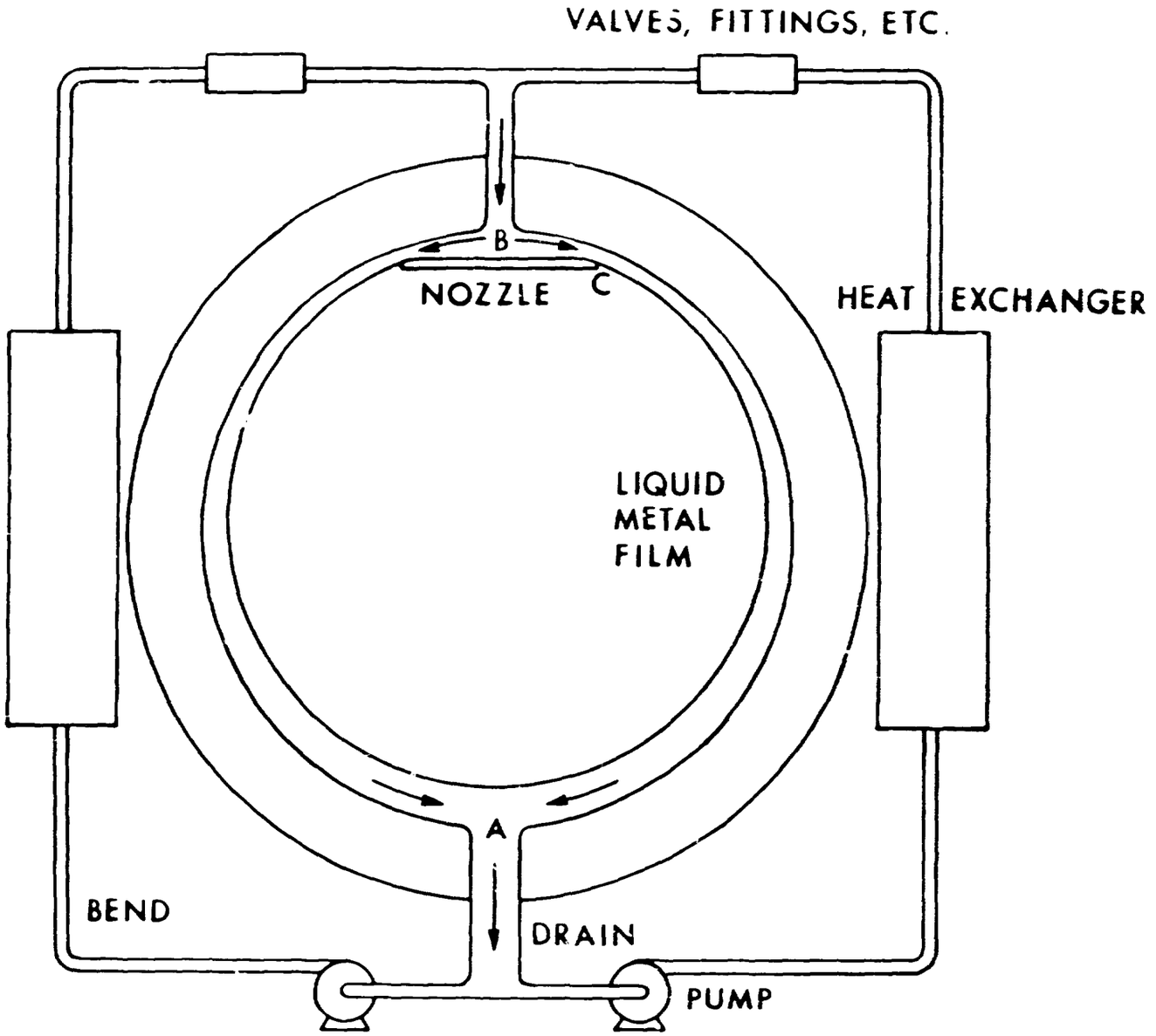
VALVES, FITTINGS, ETC.
B
NOZZLE
C
HEAT EXCHANGER
LIQUID METAL FILM
A
BEND
DRAIN
PUMP

Fig. 5